T CELLS

Long-lived T follicular helper cells retain plasticity and help sustain humoral immunity

Marco Künzli[1]*, David Schreiner[1]*, Tamara C. Pereboom[1], Nivedya Swarnalekha[1], Ludivine C. Litzler[1], Jonas Lötscher[2], Yusuf I. Ertuna[3], Julien Roux[2,4], Florian Geier[2,4], Roman P. Jakob[5], Timm Maier[5], Christoph Hess[2,6], Justin J. Taylor[7], Carolyn G. King[1†]

CD4$^+$ memory T cells play an important role in protective immunity and are a key target in vaccine development. Many studies have focused on T central memory (T_{cm}) cells, whereas the existence and functional significance of long-lived T follicular helper (T_{fh}) cells are controversial. Here, we show that T_{fh} cells are highly susceptible to NAD-induced cell death (NICD) during isolation from tissues, leading to their underrepresentation in prior studies. NICD blockade reveals the persistence of abundant T_{fh} cells with high expression of hallmark T_{fh} markers to at least 400 days after infection, by which time T_{cm} cells are no longer found. Using single-cell RNA-seq, we demonstrate that long-lived T_{fh} cells are transcriptionally distinct from T_{cm} cells, maintain stemness and self-renewal gene expression, and, in contrast to T_{cm} cells, are multipotent after recall. At the protein level, we show that folate receptor 4 (FR4) robustly discriminates long-lived T_{fh} cells from T_{cm} cells. Unexpectedly, long-lived T_{fh} cells concurrently express a distinct glycolytic signature similar to trained immune cells, including elevated expression of mTOR-, HIF-1–, and cAMP-regulated genes. Late disruption of glycolysis/ICOS signaling leads to T_{fh} cell depletion concomitant with decreased splenic plasma cells and circulating antibody titers, demonstrating both unique homeostatic regulation of T_{fh} and their sustained function during the memory phase of the immune response. These results highlight the metabolic heterogeneity underlying distinct long-lived T cell subsets and establish T_{fh} cells as an attractive target for the induction of durable adaptive immunity.

INTRODUCTION

Vaccination and infection lead to the generation of protective immune responses mediated by memory T and B cells (*1*). Two major subsets of memory T cells have been described on the basis of differential expression of lymphoid homing receptors: CCR7$^+$ central memory (T_{cm}) cells and CCR7$^-$ effector memory (T_{em}) cells (*2*). After challenge infection, T_{cm} cells produce interleukin-2 (IL-2) and maintain the capacity to proliferate and generate secondary effector cells. In contrast, T_{em} cells can immediately produce inflammatory cytokines but have more limited expansion. In addition to these subsets, CD4$^+$ T follicular helper (T_{fh}) memory cells can promote secondary B cell expansion and class switching (*3*–*7*). The number of circulating T_{fh} cells correlates with the number of blood plasmablasts after vaccination in humans and can be boosted to improve long-lived antibody production (*8*–*10*). These data suggest targeted generation of long-lived T_{fh} cells as a rational approach for improving vaccine design. However, despite the importance of T_{fh} cells for supporting antibody responses, the signals promoting maintenance and survival of these cells are not well understood. In addition, it is unclear whether T_{fh} cells retain the capacity to differentiate into diverse secondary effectors (*3*, *5*, *6*, *11*). Analysis of long-lived T_{fh} cells is complicated by a gradual loss of phenotypic markers typically associated with T_{fh} effector cells, including programmed cell death protein 1 (PD1) and CXCR5, as well as the apparent decline of the CD4$^+$ memory compartment compared with CD8$^+$ memory cells over time (*3*, *6*, *12*–*14*). Moreover, the relationship between T_{cm} cells and T_{fh} effector cells, which share several surface markers and transcription factors including CXCR5, inducible T-cell costimulator (ICOS), T cell factor 1 (TCF1), signal transducers and activators of transcription 3 (STAT3), and DNA-binding protein inhibitor ID-3 (ID3), is not well established (*3*, *15*–*19*). Recently, a T_{cm} precursor signature, including markers for lymphoid homing (*Ccr7*) and survival (*Bcl2*), was identified among antigen-specific effector cells responding to viral infection (*20*). This signature, however, was not detected in T_{fh} effector cells, suggesting an early divergence between precursors of T_{cm} and long-lived T_{fh}. Nevertheless, it remains unclear whether T_{fh} cells found at later phases are remnants of a primary effector response or whether they represent a distinct population of self-renewing T_{cm} cells that share differentiation requirements and phenotypic characteristics with T_{fh} cells.

Although informative, T cell receptor (TCR) transgenic models used to unravel these questions demonstrate intrinsically biased differentiation tendencies and may not reveal the full palette of CD4$^+$ heterogeneity (*21*). In addition, many such studies require transferring high numbers of donor cells, which could affect T cell differentiation (*3*, *22*). Using tetramers to study the polyclonal T cell response, we determined that T_{fh} cells are particularly susceptible to nicotinamide adenine dinucleotide (NAD)–induced cell death (NICD) during isolation. By blocking NICD, we observed that T_{fh} cells persist in high numbers to at least 400 days after infection, whereas T_{cm} cells decline. Transcriptional and epigenetic profiling revealed that long-lived T_{fh} cells constitutively engage glycolytic metabolism while remaining stem-like. Consistent with these findings, transfer experiments revealed that long-lived T_{fh} cells, but not T_{cm} cells, can generate the full spectrum of secondary effectors. Although long-lived T_{fh} cells

[1]Immune Cell Biology Laboratory, Department of Biomedicine, University of Basel, University Hospital Basel, CH-4031 Basel, Switzerland. [2]Department of Biomedicine, University of Basel, University Hospital Basel, CH-4031 Basel, Switzerland. [3]Department of Biomedicine, University of Basel, CH-4031 Basel, Switzerland. [4]Swiss Institute of Bioinformatics, Basel, Switzerland. [5]Biozentrum, University of Basel, Basel, Switzerland. [6]Department of Medicine, CITIID, University of Cambridge, Cambridge, UK. [7]Vaccine and Infectious Disease Division, Fred Hutchinson Cancer Research Center, Seattle, WA, USA.
*These authors contributed equally as first authors.
†Corresponding author. Email: carolyn.king@unibas.ch

can survive in the absence of antigen, they depend on sustained ICOS signals to preserve glycolytic and Tcf7-dependent gene expression. A reduction in T_{fh} cell numbers induced by late ICOS blockade led to a reduction in circulating antibody titers and splenic plasma cells, highlighting an underestimated contribution of long-lived T_{fh} cells to late phase humoral immune responses.

RESULTS

T_{fh} cells are susceptible to death during isolation

T_{fh} cells were recently described to express high levels of the purinergic receptor P2X7 receptor (*23*, *24*). P2X7R is an adenosine 5′-triphosphate–gated cation channel that can be adenosine 5′-diphosphate ribosylated by the cell surface enzyme ARTC2.2, rendering certain cell types, including regulatory T cells and resident memory T (T_{rm}) cells, susceptible to NICD during isolation from the tissue (*25*, *26*). Injection of an ARTC2.2-blocking nanobody (NICD protector) before organ harvest protects these subsets from NICD and improves their recovery from lymphoid organs (*27*, *28*). To determine whether inhibition of ARTC2.2 could also improve the recovery of T_{fh} cells at effector and memory time points, we harvested antigen-specific T cells from NICD protector–treated mice after infection with lymphocytic choriomeningitis virus (LCMV). Polyclonal LCMV-specific $CD4^+$ T cells were enriched using tetramer staining for IA^b:nucleoprotein $(NP)_{309–328}$ (NP specific) or IA^b:glycoprotein $(GP)_{66–77}$ (GP66 specific) and analyzed for expression of T_{fh}-associated surface markers; a variety of gating strategies was used to place the results in the context of previous studies assessing LCMV-induced T_{fh} cells (*3*, *12*). In untreated mice, T_{fh} effector cells were clearly identified at day 15 after infection but were largely absent by day 43 (Fig. 1A and fig. S1A). In contrast, treatment with NICD protector resulted in a significant recovery of T_{fh} cells at all time points and with both T cell specificities, indicating a larger expansion and more prolonged survival of T_{fh} cells than previously appreciated (Fig. 1, A to C). As the number of GP66-specific T_{fh} cells was about fourfold higher than NP-specific T_{fh} cells, we focused subsequent analyses on the GP66-specific T cell compartment (fig. S1B). Two-dimensional visualization of the cytometry data by *t*-distributed stochastic neighbor embedding (*t*SNE) confirmed that NICD protector preferentially rescued cells with high expression of P2X7R (Fig. 1B). NICD protector also significantly improved the recovery of P-selectin glycoprotein ligand-1 $(PSGL1)^{hi}Ly6C^{lo}$ memory cells but had minimal impact on more terminally differentiated $PSGL1^{hi}Ly6C^{hi}$ (hereafter T_H1) memory cells, in line with the levels of P2X7R expression on these subsets (Fig. 1, C and D, and fig. S1C). In addition, NICD protector improved the recovery of $Ly6c^{lo}$ and $CXCR5^+$ cells after infection with *Listeria monocytogenes*, again correlating with P2X7R expression (fig. S1, D to G). After day >400, T_{fh} cells identified by all gating strategies persisted in LCMV-infected mice, whereas $Ly6C^{lo}PSGL1^{hi}$ memory cells, a heterogeneous population previously shown to contain a substantial proportion of T_{cm}, were nearly absent (Fig. 1, A and C, and fig. S1C) (*12*). These data suggest either a survival defect or conversion of $Ly6C^{lo}PSGL1^{hi}$ memory into one of the remaining memory cell subsets. T_{fh} cells isolated at late time points after infection were further phenotyped by flow cytometry and characterized by high expression of folate receptor 4 (FR4), CD73, CXCR4, ICOS, and Bcl6 compared with T_H1 and $Ly6C^{lo}PSGL1^{hi}$ memory cells (Fig. 1D). Although a similar phenotype was observed on polyclonal NP-specific T_{fh} cells isolated from LCMV-infected mice (fig. S1A), experiments using monoclonal T cells from NICD-protected SMARTA or NIP TCR transgenic strains generated substantially fewer long-lived T_{fh} cells (fig. S1H). These observations agree with previous reports showing a gradual decline of T_{fh}-associated markers on transferred monoclonal populations and highlight the value of studying polyclonal responses, particularly given the tendency of different types of TCR transgenic T cells to undergo distinct and more limited patterns of differentiation (*3*, *12*, *21*).

FR4 discriminates long-lived T_{fh} from transcriptionally distinct T_{cm}

To further investigate $CD4^+$ T cell heterogeneity and regulation at memory time points, we performed single-cell RNA sequencing (scRNA-seq) on GP66-specific T cells isolated at day >35 after infection. To assess the effect of NICD protector using a transcriptional readout, we sequenced cells from NICD protector–treated and untreated mice and found that treatment leads to an increase in proportions of T_{fh}-like clusters (fig. S2A). To ensure consistency with other experiments, we performed further scRNA-seq analyses using the run with NICD protector. Principal components analysis (PCA) was used for dimension reduction, hierarchical clustering of the cells, and *t*SNE visualization (Fig. 2A and fig. S2B). Seven distinct clusters were enriched for genes associated with the following: T_{fh} cells (clusters 1 to 3, 37% of cells), T_{cm} cells (clusters 4 and 5, 45% of cells), and T_H1 cells (clusters 6 and 7, 18% of cells) (Fig. 2, A and B, and fig. S2B). The top defining genes in the T_{fh} clusters included established T_{fh} markers such as *Izumo1r*, *Pdcd1*, and *Sh2d1a*, as well as transcription factors expressed by $CD4^+$ memory cells, including *Klf6*, *Jun*, and *Junb* (Fig. 2, B and C) (*23*, *29*). T_{cm} and T_H1 clusters (4 to 7) exhibited higher expression of *Il7r*, *S100a4*, *S100a6*, *Selplg*, and various integrins (Fig. 2, B and D), whereas clusters 6 and 7 were enriched for genes associated with T_H1 differentiation including *Cxcr6*, *Ccl5*, *Nkg7*, and *Id2* (Fig. 2, B and E). Among T_H1 clusters, cluster 7 represented the subset highest in *Selplg*, *Ly6c2*, and *Il7r*, whereas cluster 6 expressed higher levels of *Cxcr6* and *Id2* along with signatures of dysfunction and exhaustion (fig. S2, C to E) (*20*, *30*). Cluster cell type identities were confirmed by scoring each cell for signature genes obtained from publicly available datasets and examining the scores across clusters (Fig. 2F and fig. S2F). T_{fh} and T_H1 signatures matched well with clusters 1 to 3 and 6 to 7, respectively, whereas clusters 4, 5, and 7 were enriched for the T_{cm} precursor signature reported by Ciucci *et al.* (*20*) (Fig. 2F).

Within T_{fh} clusters 1 to 3, we observed stable expression of *Izumo1r*, which encodes FR4. Although the function of this receptor on T cells is not well understood, it has been shown to be expressed on T_{fh} effector and memory cells, as well as on anergic and regulatory $CD4^+$ T cells (*23*, *31*, *32*). Compared with *Cxcr5* and *Pdcd1*, *Izumo1r* served as a much cleaner transcriptional marker of the boundary between T_{fh} and non-T_{fh} cells (Fig. 2, G and H). Unlike *Izumo1r*, *Cxcr5* expression was also detected in non-T_{fh} clusters, although with a slight decrease from T_{cm} to T_H1 (Fig. 2H). These findings were confirmed at the protein level, where $CXCR5^{hi}$ gating includes both $FR4^{hi}$ and $FR4^{lo}$ cells, whereas $FR4^{hi}$ gating largely excludes $CXCR5^{lo}$ cells (Fig. 2K). Unexpectedly, *Ccr7* expression, highest in clusters 4 and 5, was negatively correlated with *Cxcr5* in cells from animals treated with NICD protector (in the bottom 4% of all genes), whereas cells from untreated animals showed a slight positive correlation (in the top 27% of all genes) (Fig. 2G). This trend was mainly driven by

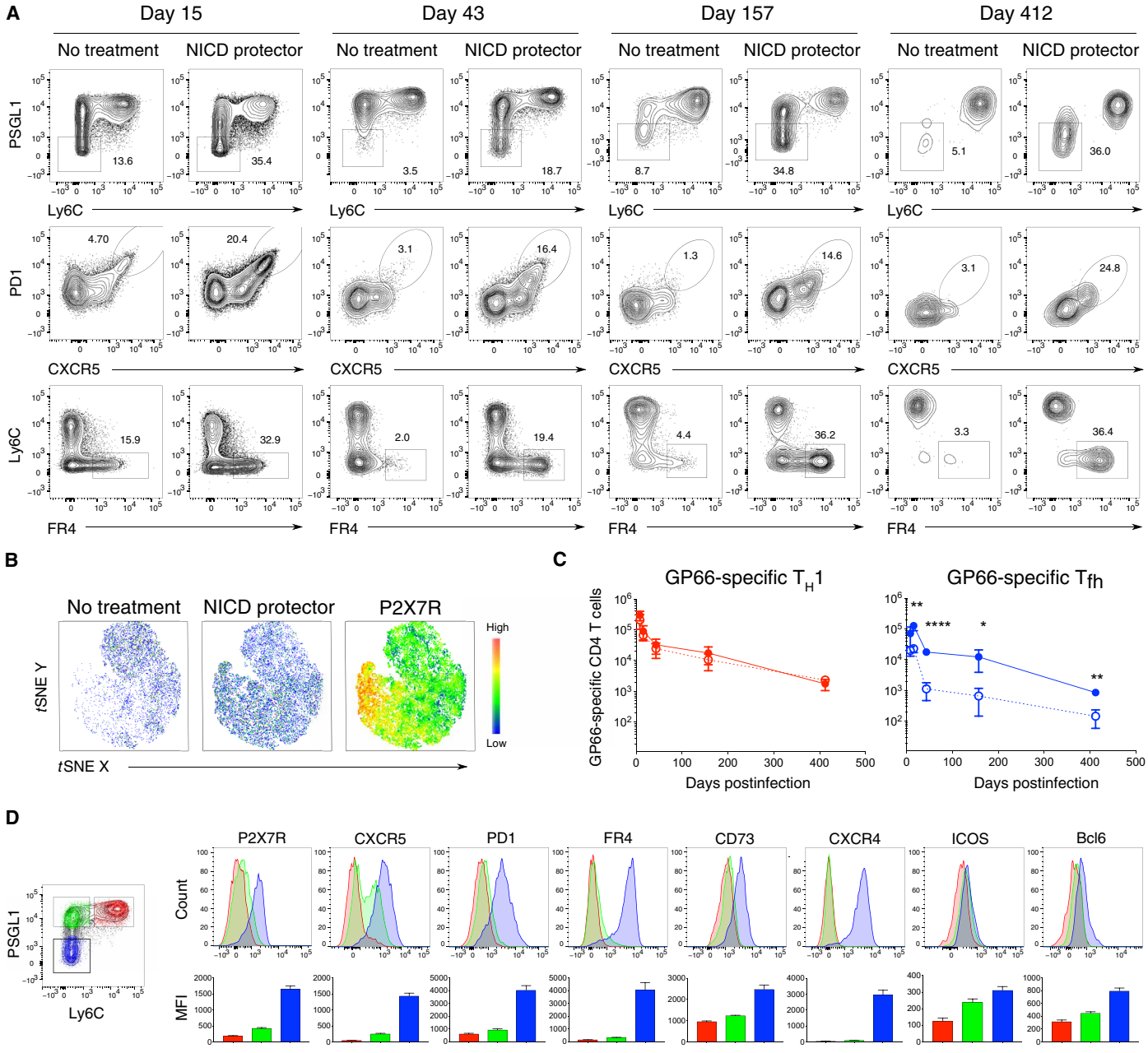

Fig. 1. T_{fh} cells are susceptible to death during isolation. (**A**) Flow cytometry analysis of GP66-specific $CD4^+$ T cells isolated from the spleen at indicated time points after infection, with or without NICD protector using different gating strategies to identify long-lived T_{fh} cells ($Ly6C^{lo}PSGL1^{lo}$, $CXCR5^{hi}PD1^{hi}$, or $FR4^{hi}Ly6C^{lo}$). (**B**) *t*SNE plots of the GP66-specific $CD4^+$ memory compartment with (middle and right) or without NICD protector (left) and overlaid P2X7R expression with red indicating the highest expression level (right). (**C**) Quantification of GP66-specific T_H1 memory (red, $Ly6C^{hi}PSGL1^{hi}$) or long-lived T_{fh} cell (blue, $Ly6C^{lo}PSGL1^{lo}$) numbers over time with (solid lines) or without (dashed lines) NICD protector gated as in Fig. 1D. Thin lines represent the means ± SD. (**D**) Representative flow cytometry plots and geometric mean fluorescence intensity (hereafter MFI) of the indicated marker in GP66-specific $CD4^+$ memory cell subsets T_H1 (red), $Ly6C^{lo}PSGL1^{hi}$ (green), and T_{fh} (blue) >40 days after infection. Data represent $N = 2$ independent experiments for (D) with $n = 3$ to 5 mice per group. Unpaired two-tailed Student's *t* test was performed on each individual time point (C). $^*P < 0.05$, $^{**}P < 0.01$, $^{****}P < 0.0001$.

the bona fide T_{fh} clusters (1 to 3) preferentially rescued from NICD, as illustrated by imputed expression levels of *Cxcr5* versus *Ccr7* (Fig. 2I). A similar negative correlation was found between protein expression levels for CCR7 and CXCR5, with the highest CCR7-expressing cells falling within the $Ly6C^{lo}PSGL1^{hi}$ (hereafter T_{cm}) compartment (Fig. 2J and fig. S2G). Long-lived GP66-specific T_{fh} cells found in lymph nodes also expressed lower levels of CCR7 compared with T_{cm}, consistent with the idea that T_{fh} cells generated in lymphoid organs are a noncirculating population similar to resident memory cells (fig. S2H) (*33*). T_{fh} cells have a higher expression of CD69 and enrichment for residency-associated genes (fig. S2, I and J) (*34*–*36*). Together, the use of FR4 as a marker for long-term T_{fh} identity

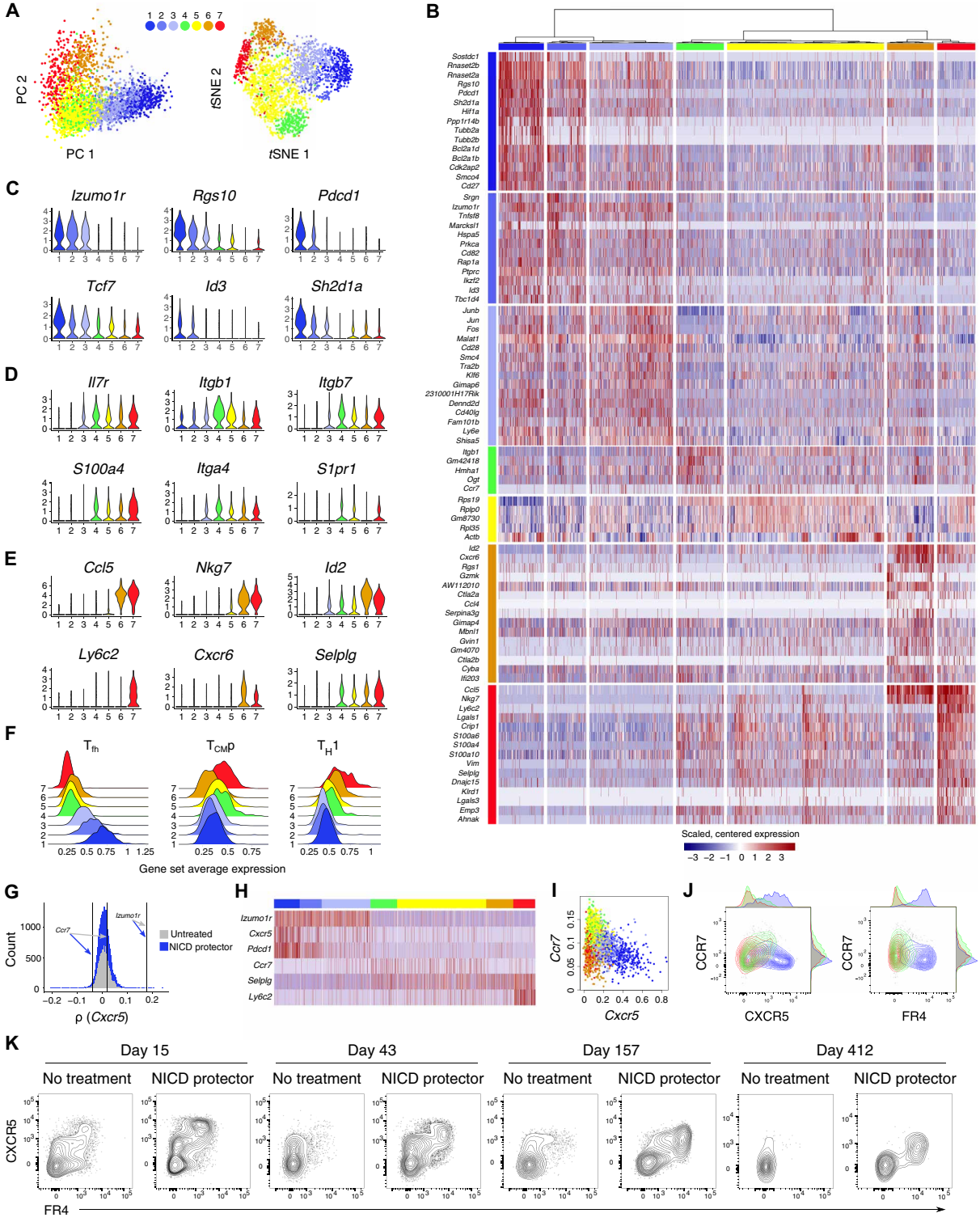

Fig. 2. FR4 discriminates long-lived T_{fh} from transcriptionally distinct T_{cm}. (**A**) Unsupervised hierarchical clustering using Ward's method: PCA and *t*SNE dimension reductions. (**B**) Heatmap showing scaled, centered single-cell expression of top 15 genes sorted according to cluster average log fold change (FC) , adjusted *P* value of <0.05. (**C** to **E**) Log-normalized expression of genes typical for T_{fh} (C), T_{cm} (D), and T_H1 (E) populations. (**F**) Log-normalized average expression of published $CD4^+$ signatures obtained by analysis of d7 effectors: T_{fh}, T_{cm} precursors, and T_H1. (**G**) scRNA-seq: Rank of *Ccr7* and *Izumo1r* (encoding FR4) among Spearman's rank correlation coefficients between *Cxcr5* and all other genes, NICD protector versus untreated. (**H**) Scaled, centered single-cell expression of *Izumo1r* in comparison with other common gating markers. (**I**) scRNA-seq: Cxcr5 versus Ccr7 on imputed data, colored by cluster. Dropout imputed using Seurat::AddImputedScore. (**J** and **K**) Flow cytometry analysis of CCR7, CXCR5, and FR4 on GP66-specific $CD4^+$ memory subsets >50 days after infection gated as in Fig. 1D (J) or at the indicated time points after infection, with or without NICD protector (K). Data represent $N = 2$ independent experiments with $n = 4$ mice (J).

improves upon previous gating strategies, which either allocate too many T_{cm} cells into a T_{fh} gate or depend upon markers like PD1, which is known to decline over time. We additionally noted that *Hif1a*, a transcription factor normally associated with glycolysis, was one of the top genes expressed by T_{fh} cells, consistent with the recently reported enrichment of this transcription factor in T_{fh} effectors and resident memory cells (Fig. 2B) (*37*–*39*). Together, these data highlight clear transcriptional distinctions between T_{cm} cells and the ultimately more persistent NICD-rescued T_{fh} cells.

Long-lived T_{fh} cells are constitutively glycolytic

In addition to *Hif1a* expression, long-lived T_{fh} cells were enriched for mammalian target of rapamycin (mTOR)– and cyclic adenosine 3′,5′-monophosphate (cAMP)–regulated genes, suggesting a metabolic signature similar to that observed in trained immune cells (Fig. 3A and fig. S3, A to C) (*40*–*44*). Enhanced activation of mTOR-regulated genes was also observed in secondary analysis of microarray data on bulk sorted SMARTA T_{fh} memory cells (where PD1 protein expression was negative) and in recently published single-cell data from GP66-specific T_{fh} memory cells (fig. S3, D and E) and was further confirmed by quantitative polymerase chain reaction (qPCR) of mTOR-regulated genes in sorted $CD4^+$ GP66-specific memory T cell populations (Fig. 3B) (*3*, *20*, *43*). These data indicate that long-lived T_{fh} cells may constitutively engage a glycolytic metabolism. To assess mTORC1 activity, we measured phosphorylation of TORC1 target ribosomal protein S6 (p-S6) directly after T cell isolation (Fig. 3C and fig. S3F). Both GP66-specific T_{fh} cells and $CD44^+$ T_{fh} cells, which are phenotypically similar to antigen-specific T_{fh} cells (fig. S3G), exhibited increased p-S6 compared with T_H1 memory cells (Fig. 3C and fig. S3F). To exclude modulation of p-S6 due to tetramer-induced activation, we conducted experiments on ice with dasatinib, a tyrosine kinase inhibitor shown to temporarily block TCR-mediated signal transduction (*45*). Consistent with mTOR activation, long-lived T_{fh} cells had increased uptake of the fluorescent glucose analog 2-(*N*-(7-nitrobenz-2-oxa-1,3-diazol-4-yl)amino)-2-deoxyglucose) (2-NBDG) and an increased baseline extracellular acidification rate (ECAR) compared with T_H1 memory cells (Fig. 3, D and E). However, alongside this apparent increase in glycolytic metabolism, long-lived T_{fh} cells had slightly decreased expression of the amino acid transporter CD98 and the transcription factor c-myc (classically viewed as activation markers) compared with T_H1 memory cells, indicating that not all measures of anabolic activity are increased (Fig. 3, F and G).

To determine whether the shift toward glycolysis by long-lived T_{fh} cells was accompanied by a reduction in oxidative metabolism, we also assessed their baseline oxygen consumption rate (OCR). Although we observed a slight reduction in basal respiration by long-lived T_{fh} cells compared with T_H1 memory cells, the maximum respiration and spare respiratory capacity were similar between these two populations (Fig. 3H). Transcriptionally, long-lived T_{fh} cells were also enriched for genes associated with oxidative phosphorylation and mitochondrial respiration, a signature associated with $CD8^+$ memory T cell survival (fig. S3H). Because T_{fh} effectors were previously reported to have decreased mTOR activation and reduced glycolysis (*46*), we also assessed the metabolic capacity of cells isolated at day 10 after infection, reasoning that NICD protector might improve their survival and fitness. At this time point, T_{fh} effectors had slightly reduced basal ECAR compared with T_H1 effectors but demonstrated normal glycolytic flux after the addition of carbonyl cyanide *p*-trifluoromethoxyphenylhydrazone (Fig. 3I). Similar to long-lived T_{fh} cells, T_{fh} effectors had equivalent baseline and maximal respiratory capacity to T_H1 effectors, indicating that in contrast to an earlier report, T_{fh} cells isolated at earlier time points are also metabolically fit (Fig. 3J) (*12*). To test whether these discrepancies can be explained by the effect of NICD protector, we compared cell viability and 2-NBDG uptake with or without NICD protector from T cells isolated at days 10 (effector) and 110 (memory) after infection. NICD protector predominantly improved the viability of the T_{fh} subset as measured by annexin V staining (fig. S3, I and J). In addition, annexin V–negative T_{fh} cells from unprotected mice failed to take up 2-NBDG, demonstrating a fundamental metabolic difference from NICD-protected T_{fh} cells (fig. S3K). These results indicate that both T_{fh} effector and memory cells have greater metabolic capacity than previously appreciated.

To assess whether glycolysis/mTOR signaling are required to maintain long-lived T_{fh} cells, we examined T_{fh} cell survival in mice treated with the glycolysis inhibitor 2-deoxyglucose (2-DG) and rapamycin starting at day >40 after LCMV infection. After 2 weeks of 2-DG/rapamycin treatment, both the proportion and number of long-lived T_{fh} cells were significantly decreased, with the remaining T_{fh} cells showing reduced size consistent with less mTOR activation (Fig. 3, K and L, and fig. S3L) (*46*). Signaling through P2X7R was recently suggested to restrain mTOR activation, leading to improved survival of $CD8^+$ memory T cells (*47*). In contrast, P2X7R signals have been shown to restrain accumulation of T_{fh} effectors in Peyer's patches (*24*). To assess whether P2X7R signals promote or restrain long-lived T_{fh} cell survival, we generated radiation bone marrow chimeras with a mixture of wild-type and P2X7R-deficient bone marrow. Sixty days after LCMV infection, P2X7R-deficient T cells generated an increased proportion of all memory cells, with the most significant increase in the T_{fh} compartment (Fig. 3, M and N). These data demonstrate that P2X7R is a key negative regulator of long-lived T_{fh} cell accumulation and are consistent with a role for P2X7R in restraining mTOR activation.

Antigen is not required for the survival of long-lived T_{fh} cells

Glycolytic metabolism in T cells is often associated with activation and effector cell proliferation. To understand whether long-lived T_{fh} cells are responding to ongoing antigen stimulation, we examined Nur77 expression in LCMV-infected Nur77 reporter mice. About 30% of $PSGL1^{lo}Ly6C^{lo}$ T_{fh} cells were Nur77 positive, with a slightly higher percentage in the $CXCR5^{hi}PD1^{hi}$ T_{fh} compartment (Fig. 4A). Whereas PD1 expression was moderately increased on $Nur77^+$ compared with $Nur77^-$ T_{fh} cells, it was much higher in both of these populations than in non-T_{fh} cells (Fig. 4B). Although these data indicate that a fraction of the long-lived T_{fh} compartment continues to respond to antigen, we did not observe a positive correlation between PD1 expression and 2-NBDG uptake. Glucose uptake within the T_{fh} compartment is thus unlikely to be related to antigen stimulation (fig. S4A). Furthermore, increased 2-NBDG uptake was maintained by long-lived T_{fh} cells at >400 days of infection, by which time PD1 expression by T_{fh} cells has decreased (fig. S4B). To understand whether the glycolytic metabolism observed in long-lived T_{fh} cells is related to proliferation, we administered bromo-2′-deoxyuridine (BrdU) in the drinking water of LCMV-infected mice beginning 40 days after infection. After 12 to 14 days, about 4 to 9% of T_{fh} cells incorporated BrdU, with a slightly higher proportion of $CXCR5^{hi}PD1^{hi}$ T_{fh} cells staining positive (Fig. 4C). FR4-negative

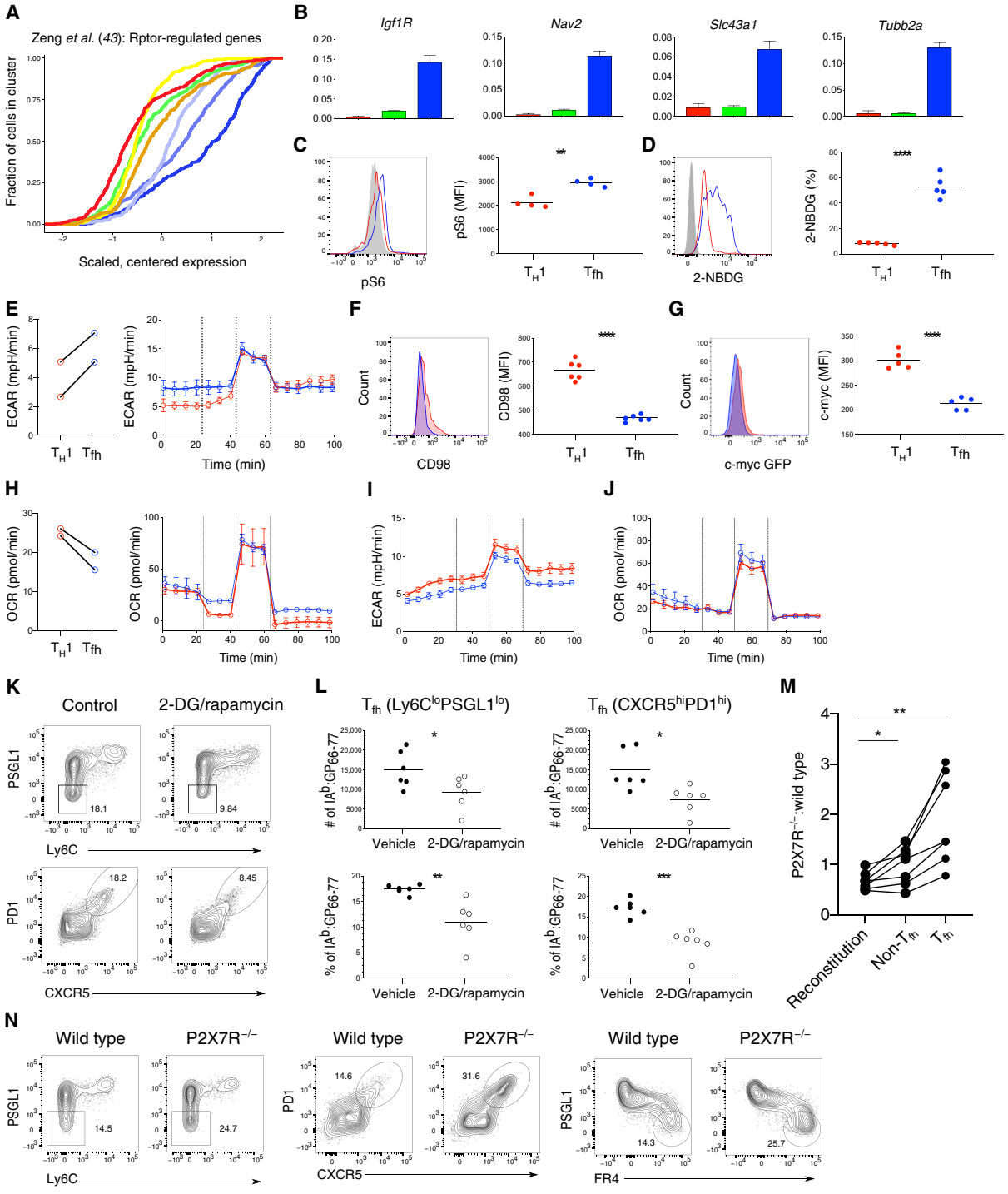

Fig. 3. Long-lived T_{fh} cells are constitutively glycolytic. (**A**) Cumulative distribution of scaled, centered mRNA expression of Rptor-regulated genes by cluster (*43*). (**B**) qPCR of genes (arbitrary units relative to Rpl13a) in sort-purified GP66-specific T_H1 memory (red), T_{cm} (green), and long-lived T_{fh} (blue) cells gated as in Fig. 1D. (**C** and **D**) Representative histograms and quantification of phospho-S6 Ser240/244 on long-lived CD44$^+$ T_H1 or T_{fh} cells compared with naïve CD4$^+$ T cells (gray) (C) and 2-NBDG uptake (D) on GP66-specific cells >30 days after infection compared with unstained control (gray). (**E**) Basal ECAR and ECAR profile in response to Mito Stress test in T_H1 memory and long-lived T_{fh} cells pooled from 20 to 30 mice. (**F** and **G**) Histogram and MFI of CD98 (F) or c-myc GFP (G) in GP66-specific memory T_H1 and long-lived T_{fh}. (**H**) Basal respiration and OCR profile in response to Mito Stress test on sorted CD44$^+$ T_H1 memory and long-lived T_{fh}. (**I** and **J**) ECAR profile (I) and OCR profile (J) in response to Mito Stress test in T_H1 and T_{fh} effector cells (day 10 after infection) pooled from $n = 12$ to 14 mice. Representative flow cytometry plots (**K**) and quantification (**L**) of GP66-specific cells treated with vehicle or 2-DG/rapamycin. (**M** and **N**) P2X7R$^{-/-}$ to wild-type ratio of GP66-specific T_{fh} cells >60 days after infection (M) and analysis (**N**) using different gating strategies. Data are representative of $N = 2$ independent experiments depicting the means ± SD of $n = 3$ technical replicates (B) or 4 to 7 mice per group [(C) to (G) and (K) to (N)]. Dots represent cells from individual mice, and the line represents the mean. Unpaired (C, D, F, G, and L) or paired (M) two-tailed Student's *t* test was performed with *$P < 0.05$, **$P < 0.01$, ***$P < 0.001$, ****$P < 0.0001$.

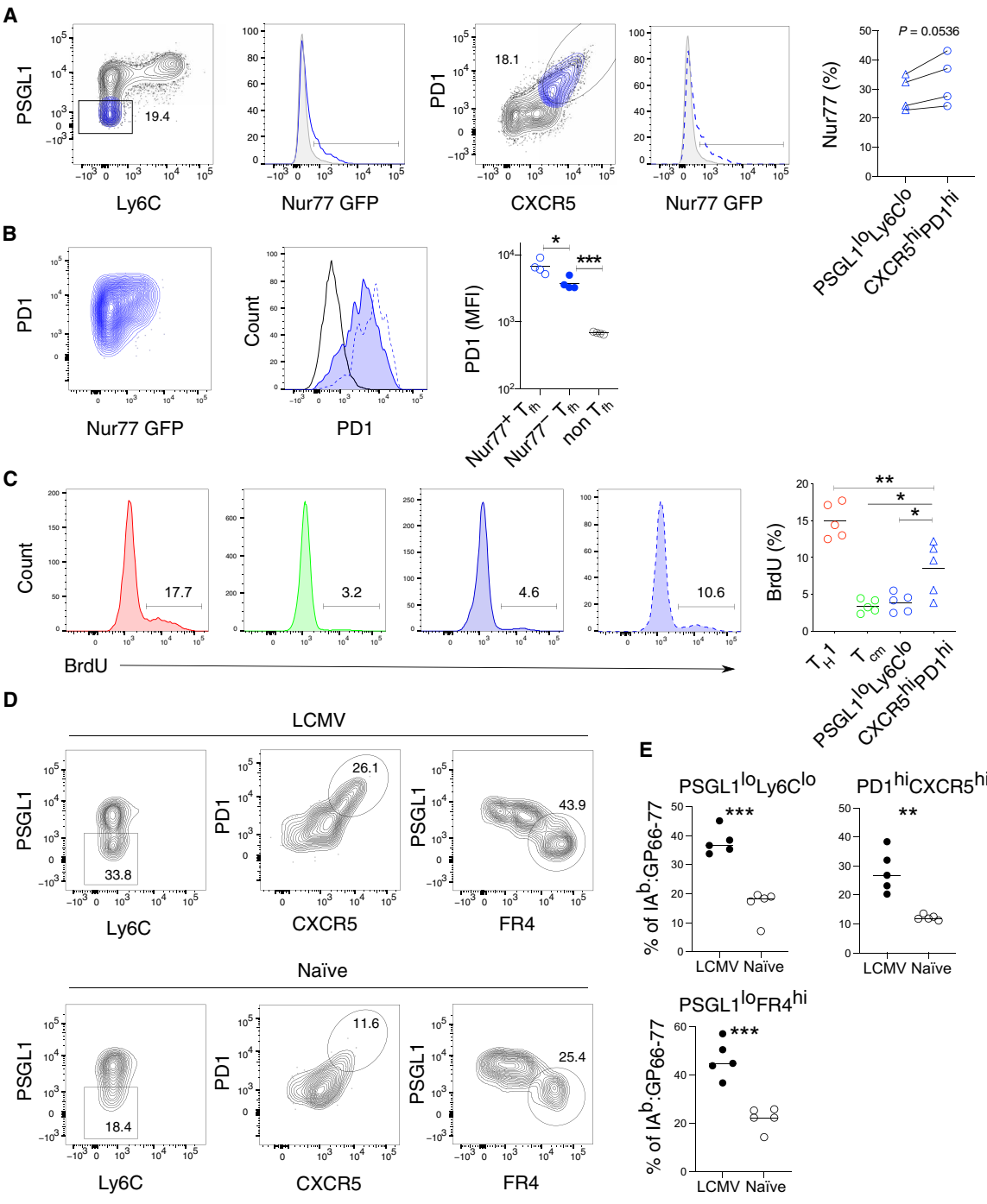

Fig. 4. Antigen is not required for the survival of long-lived T_{fh} cells. (**A**) Flow cytometry analysis of Nur77 expression by GP66-specific long-lived T_{fh} cells for the indicated gating strategies. (**B**) Representative flow cytometry plots (left) and MFI (right) depicting PD1 expression on Nur77$^+$ (blue dotted line) and Nur77$^-$ (tinted blue line) T_{fh} cells, gated as depicted in (A). (**C**) Flow cytometry plots (left) and quantification (right) of BrdU incorporation by GP66-specific CD4$^+$ memory subsets after providing BrdU for 12 days in drinking water. (**D** and **E**) Total GP66-specific CD4$^+$ T cells isolated at day 10 after LCMV infection and transferred into congenic infection-matched (LCMV) or naïve mice. Donor cell phenotype analyzed at day 30 after infection. Representative flow cytometry plots (D) and quantification (E) with gating for PSGL1^{lo} Ly6C^{lo} (left), PD1^{hi}CXCR5^{hi} (middle), and PSGL1^{lo}FR4^{hi} (right). Dots represent cells from individual mice, and the line depicts the mean. Data represent $N = 2$ independent experiments with $n = 4$ to 5 mice. Paired (A) or unpaired two-tailed Student's t test (B, C, and E) was performed with $^*P < 0.05$, $^{**}P < 0.01$, $^{***}P < 0.001$.

T_{cm} cells containing a mixture of CXCR5$^+$ and CXCR5$^-$ cells showed a similar level of in vivo cycling with about 3% of cells staining for BrdU, whereas 15% of T_H1 memory cells stained positive, demonstrating more extensive proliferation by this subset (Fig. 4C). The glycolytic phenotype observed in long-lived T_{fh} cells is thus not strongly correlated with extensive cell division, although the slightly increased BrdU incorporation by CXCR5^{hi}PD1^{hi} T_{fh} cells may be related to ongoing antigen stimulation. To better understand the contribution of antigen to maintaining the long-lived T_{fh} compartment, we transferred LCMV-specific effector cells isolated at day 10 after infection into either LCMV infection matched or naïve recipients, followed by analysis of donor T cell phenotype. Thirty days after primary infection, T_H1 memory cells were nearly absent in both transfer scenarios, indicating that T_H1 effector cells survive poorly in this setting (Fig. 4D). In contrast, GP66-specific T_{fh} cells were detected in both antigen-free (naïve) and infection-matched mice. Although fewer T_{fh} cells (with dampened expression of CXCR5 and PD1) were recovered from naïve mice, this may be partially due to ongoing expansion of T_{fh} effector cells in LCMV-infected recipients between days 10 and 15 after transfer (Figs. 1C and 4, D and E). The

long-lived donor T_{fh} cells maintained high expression of FR4 with or without antigen, consistent with scRNA-seq data identifying *Izumo1r*/FR4 as a superior marker for long-lived T_{fh} cells (Figs. 2, C and H, and 4, D and E). Together, these data indicate that although T_{fh} cells with high expression of CXCR5 and PD1 survive optimally in the presence of antigen, they nevertheless persist in its absence and without classical signs of activation or proliferation.

T_{fh} cells generate multiple cell fates upon recall

Despite maintaining a glycolytic phenotype, long-lived T_{fh} cells are enriched for genes regulated by *Tcf7* (encoding TCF1) and highly express *Cd27*, a marker associated with memory T cell survival, cytokine production potential, and stemness (Fig. 5, A and B) (*48*–*50*). Although higher expression of *Tcf7* in long-lived T_{fh} cells matched higher expression of TCF1 protein, CD27 protein expression was substantially lower in T_{fh} compared with T_H1 memory cells (Fig. 5, C and D). To determine whether the discrepancy between the CD27 gene expression and protein expression was due to P2X7R-mediated shedding, we examined CD27 on memory cells isolated from LCMV-infected mixed bone marrow chimeras reconstituted with an equal mixture of P2X7R-deficient and wild-type bone marrow cells (*51*). We observed higher expression of CD27 on P2X7R-deficient long-lived T_{fh} cells compared with both wild-type T_{fh} and T_H1 memory cells (Fig. 5D). Consistent with high expression of both *Tcf7* and *Cd27*, T_{fh} cells were also enriched for "early memory"–associated genes (fig. S5A) (*52*). In addition, construction of a cell developmental trajectory indicated that T_{fh} and T_H1 memory cells occupied opposite ends of a pseudotime trajectory, predicting enhanced differentiation plasticity in one of these subsets (Fig. 5E and fig. S5, B and C) (*53*). To test this in vivo, long-lived T_{fh} ($FR4^{hi}PSGL1^{lo}Ly6C^{lo}$), T_H1 memory ($FR4^{lo}PSGL1^{hi}Ly6C^{hi}$), and T_{cm} ($FR4^{lo}PSGL1^{hi}Ly6C^{lo}$) cells were sorted from LCMV-infected mice and transferred into naïve congenic recipients, followed by secondary challenge with LCMV (Fig. 5F). To prevent tetramer-induced activation, we stained cells for transfer in the presence of dasatinib. Twelve days after recall infection, transferred T_{fh} cells differentiated into both T_{fh} and T_H1 effectors, demonstrating lineage flexibility (Fig. 5, G and H). Consistent with a stem-like character, transferred T_{fh} donor cells also expanded most upon reactivation, generating the largest pool of each secondary effector subset (Fig. 5I). In contrast, T_{cm} cells maintained the capacity to differentiate into both $Ly6C^{hi}$ and $Ly6C^{lo}$ effectors, but generated few T_{fh} effectors, suggesting more limited plasticity (Fig. 5, G to I). Consistent with several reports, T_H1 memory cells almost exclusively gave rise to $Ly6C^{hi}$ effectors, indicating more terminal differentiation of these cells (Fig. 5, G to I) (*3*, *6*). Together, these data demonstrate that despite engaging an anabolic metabolism often associated with effector cell proliferation and differentiation, long-lived T_{fh} cells have a stem-like, early memory signature and maintain the capacity to differentiate into multiple types of effectors after secondary challenge.

Epigenetic regulation of long-lived T_{fh} cells

To assess whether the distinct transcriptional signatures observed in T_{fh} and T_H1 memory cells were also apparent at the epigenetic level, we compared chromatin accessibility of T_H1 memory, long-lived T_{fh}, and naïve T cells by assay for transposase-accessible chromatin using sequencing (ATAC-seq) (*54*). The majority of called peaks were shared among these three populations, with the highest number of unique peaks present in naïve $CD4^+$ T cells (fig. S6A). PCA revealed that T_{fh} and T_H1 memory cells are set apart from naïve T cells along PC1 yet separated from each other along PC2, indicating distinct accessibility profiles (Fig. 6A). Whereas T_H1 memory cells had more differentially open peaks annotated to exons, introns, and distal intergenic regions, long-lived T_{fh} cells had about 50% more differentially accessible peaks in promoter regions (fig. S6B). We thus focused on the significantly differentially accessible promoter regions with a high fold change ($\log_2$ fold change > 1 and false discovery rate < 0.05) between at least two of the T cell subsets and performed hierarchical clustering. This resulted in clusters of genes with common accessibility patterns: e.g., up in naïve, up in memory, and up in naïve and long-lived T_{fh} (Fig. 6B and fig. S6C). For example, the *Foxp1* promoter was exclusively accessible in naïve $CD4^+$ T cells, consistent with its role as a gatekeeper of the naïve to memory T cell transition (*55*). Integrative analysis of ATAC-seq and RNA-seq data (in silico pseudo-bulk samples derived from scRNA-seq data) revealed a correlation between the promoter accessibility and expression of genes defining T_{fh} and T_H1 memory cell subsets (Fig. 6C) (*3*). Consistent with a study that assessed the DNA methylation status of various cytokine loci in T_{fh} and T_H1 memory cells (*3*), we observed that the *Gzmb* promoter was exclusively accessible in T_H1 memory cells, whereas the *Ifny* promoter was accessible in both populations, albeit at slightly lower levels in long-lived T_{fh} cells (Fig. 6D). In contrast to this earlier study, however, the promoter accessibility of the hallmark T_{fh} cytokine, *Il21*, was restricted to long-lived T_{fh} cells (Fig. 6D). In addition, one of the most accessible cytokine promoter regions in long-lived T_{fh} cells was the epidermal growth factor–like ligand amphiregulin (*Areg*), notable for its role in restoring tissue integrity after infection (*56*). To further assess differences in the transcriptional regulation of T_{fh} and T_H1 memory cells, we analyzed enriched binding motifs in called peaks using Hypergeometric Optimization of Motif EnRichment (HOMER) (*57*). In agreement with the scRNA-seq data, long-lived T_{fh} cells were enriched for motifs belonging to the TCF transcription factor family and activating protein 1 (AP1) family members, which are known to be similarly regulated in $CD8^+$ memory cells (Fig. 6E) (*58*, *59*). In contrast, T_H1 memory peaks exhibited increased Runx and T-box transcription family member binding sites, consistent with the cooperation of these transcription factors in regulating interferon-γ and stabilizing T_H1 fate in $CD4^+$ T cells (Fig. 6F) (*60*, *61*). These observations were further validated by applying single-cell regulatory network inference and clustering to the scRNA-seq data, which highlighted TCF/AP1 and Runx family members as regulators in long-lived T_{fh} and T_H1 memory, respectively (fig. S6D). We next assessed functional pathways in the ATAC-seq data by running gene set enrichment analysis (GSEA) on differentially accessible promoter regions in long-lived T_{fh} compared with T_H1 memory cells using both standard gene set categories and sets curated from relevant publications (fig. S6E). Here, we observed increased promoter accessibility in long-lived T_{fh} cells of *Rptor*- and *Tcf7*-regulated genes and genes activated in response to *cAMP*, suggesting that the anabolic and stem signatures of this population are strongly regulated at the epigenetic level (fig. S6E).Last, using Ingenuity Pathway Analysis (Qiagen, version 01-14) to probe the functional regulation of long-lived T_{fh} cells, we identified ICOS-inducible T-cell costimulator ligand (ICOSL) signaling as one of the top pathways enriched in both ATAC-seq and scRNA-seq datasets (fig. S6F) (*62*). These data raise the possibility that ICOS-mediated signals contribute to the maintenance and identity of long-lived T_{fh} via specific epigenetic modifications.

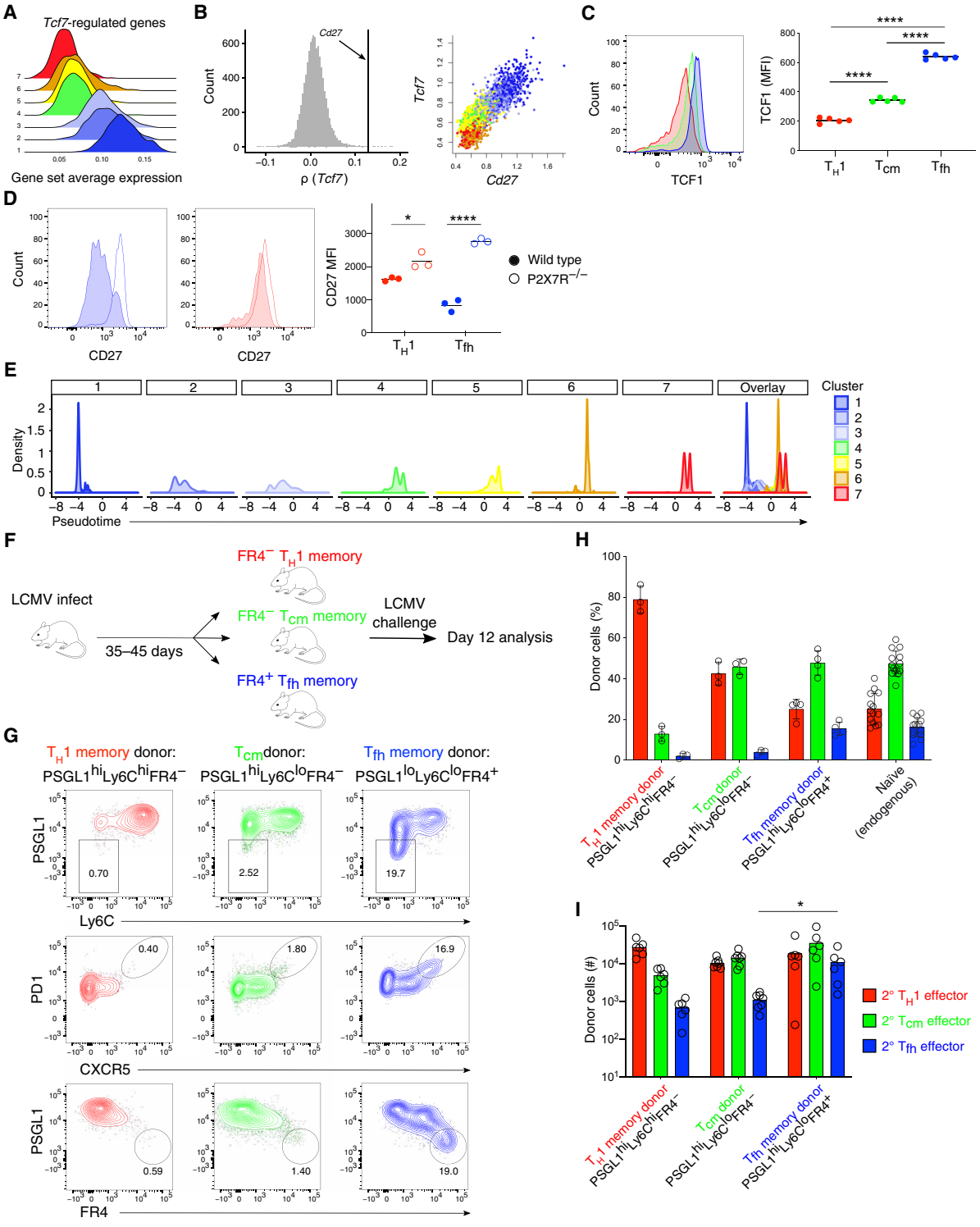

Fig. 5. T_{fh} cells generate multiple cell fates upon recall. (**A**) Log-normalized average expression of genes tracking with *Tcf7* (*90*). (**B**) scRNA-seq: Rank of *Cd27* among Spearman's rank correlation coefficients between *Tcf7* and all other genes (left). *Cd27* versus *Tcf7* on imputed data (right), colored by cluster. (**C** and **D**) Flow cytometry analysis of TCF1 (C) in wild type and CD27 (D) in mixed wild-type and P2X7R$^{-/-}$ bone marrow chimera mice in T_H1 (red), T_{cm} (green), and T_{fh} (blue) GP66-specific memory cells. (**E**) Density of cells in pseudotime using Monocle2 analysis. (**F**) GP66-specific T_H1, T_{cm}, or T_{fh} CD4$^+$ T cells sorted at days 35 to 45 after LCMV infection and transferred into congenic naïve mice. Recipient mice challenged with LCMV the following day. Donor cell phenotype analyzed at day 12 after infection. (**G**) Representative flow cytometry plots of T_H1, T_{cm}, or T_{fh} donor cell phenotype. (**H** and **I**) Quantification of proportions (H) and numbers (I) of T_H1 effectors (red), T_{cm} (green), and T_{fh} effectors (blue) from T_H1, T_{cm}, or T_{fh} donors compared with endogenous response. Data represent $N = 2$ independent experiments with $n = 5$ (C) or 3 to 14 (D to H) mice per group with the thin line depicting the mean and the dots representing cells from individual mice. (**I**) Summarizes $N = 2$ independent experiments with $n = 6$ to 7 mice. One-way analysis of variance (ANOVA) followed by Tukey's posttest for multiple comparisons (C) or unpaired two-tailed Student's *t* test (D and I) with $^*P < 0.05$ and $^{****}P < 0.0001$.

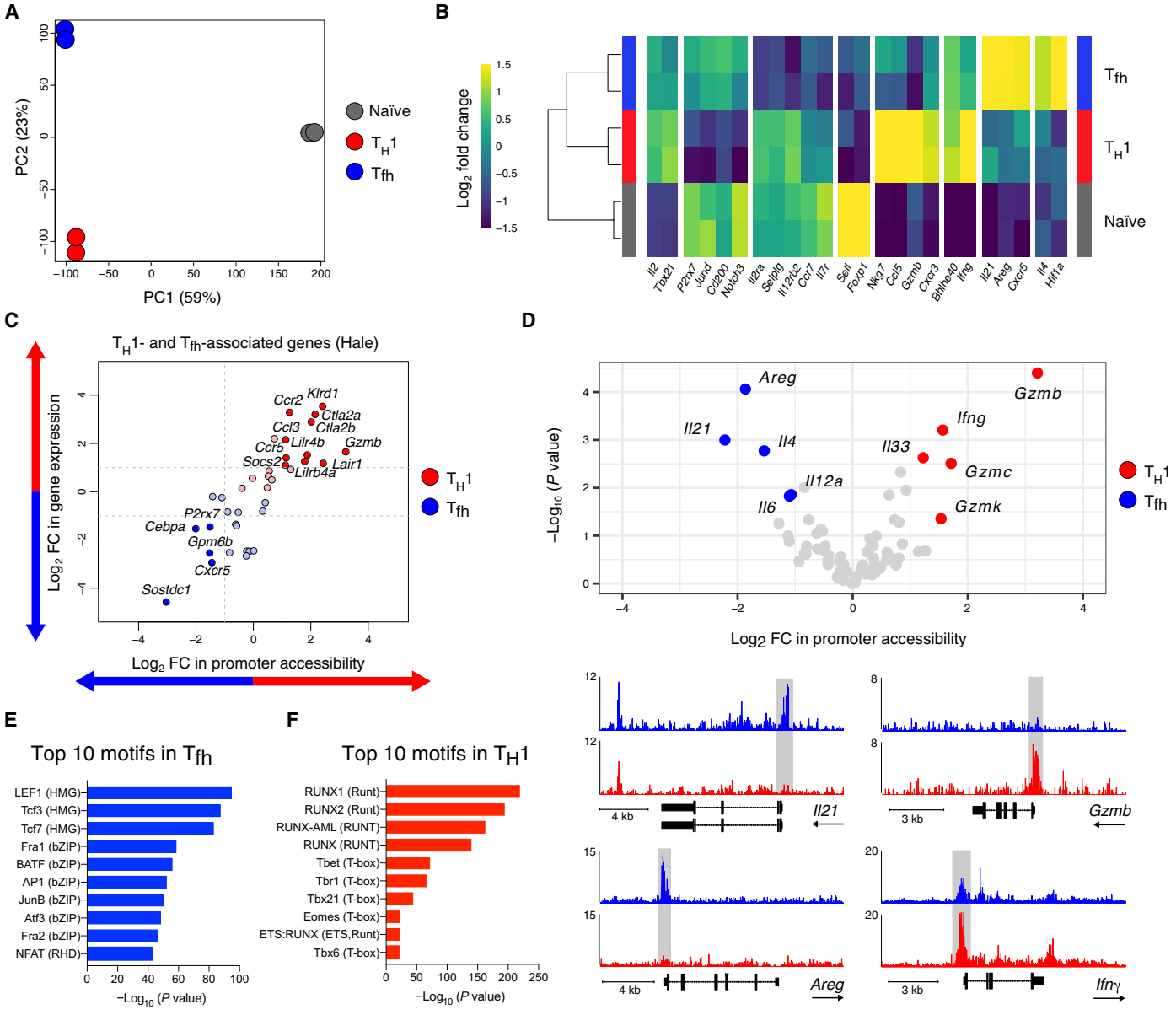

Fig. 6. Epigenetic regulation of long-lived T_{fh} cells. (**A**) PCA of ATAC-seq data on all peaks. (**B**) Heatmap of hierarchically clustered promoter regions of highlighted genes. Genes with absolute value (log_2 FC) > 1 are assigned the most extreme colors. (**C**) Scatter plots of ATAC-seq promoter log2 FC and in silico pseudo-bulk RNA-seq log_2 FC with blue and red arrows indicating enrichment in T_{fh} and T_H1 compartment, respectively. (**D**) Volcano plot of cytokine promoter region accessibility with blue and red dots indicating increased accessibility in T_{fh} and T_H1 compartment, respectively, and highlighted gene tracks. (**E** and **F**) Enriched motifs in long-lived T_{fh} (E) or T_H1 memory cells (F) found by HOMER.

ICOS signaling maintains T_{fh} cell identity at late time points

Although ICOS has an established role in primary T_{fh} responses, its role in maintaining $CD4^+$ T cells in the long term is less clear. ICOS signaling has been shown to induce the expression of *Tcf7* in Th17 memory cells that maintain the plasticity to differentiate after stimulation (*63*). ICOS can also induce mTORC1 activation in both T_{fh} effector and T follicular regulatory effector cells, leading to further stabilization of the follicular T cell program (*43*, *64*, *65*). To test the hypothesis that ICOS signals contribute to the integration of stemness and anabolic metabolism in long-lived T_{fh} cells, we treated LCMV-infected mice with anti-ICOSL starting at day >50 after infection (Fig. 7A). After 12 days of treatment, the number of GP66-specific T_{fh} cells was decreased in anti-ICOSL–treated mice (Fig. 7B). T_{fh} cells remaining after ICOS blockade had decreased expression of TCF1 and reduced activation of mTOR as measured by cell size (fig. S7, A and B). To further characterize the effects of anti-ICOSL blocking on long-lived T_{fh} cells, we performed RNA-seq at day 60 after infection on control and treated mice. Cells from mice treated with anti-ICOSL for 12 days before harvest exhibited lower transcription of key T_{fh} genes such as *Pdcd1*, *Cxcr5*, and *Bcl6*, whereas known T_H1 survival factors such as *Bcl2* and *Il7r* were increased (Fig. 7C). GSEA showed decline of T_{fh}-defining, resident memory, *Rptor*-regulated,

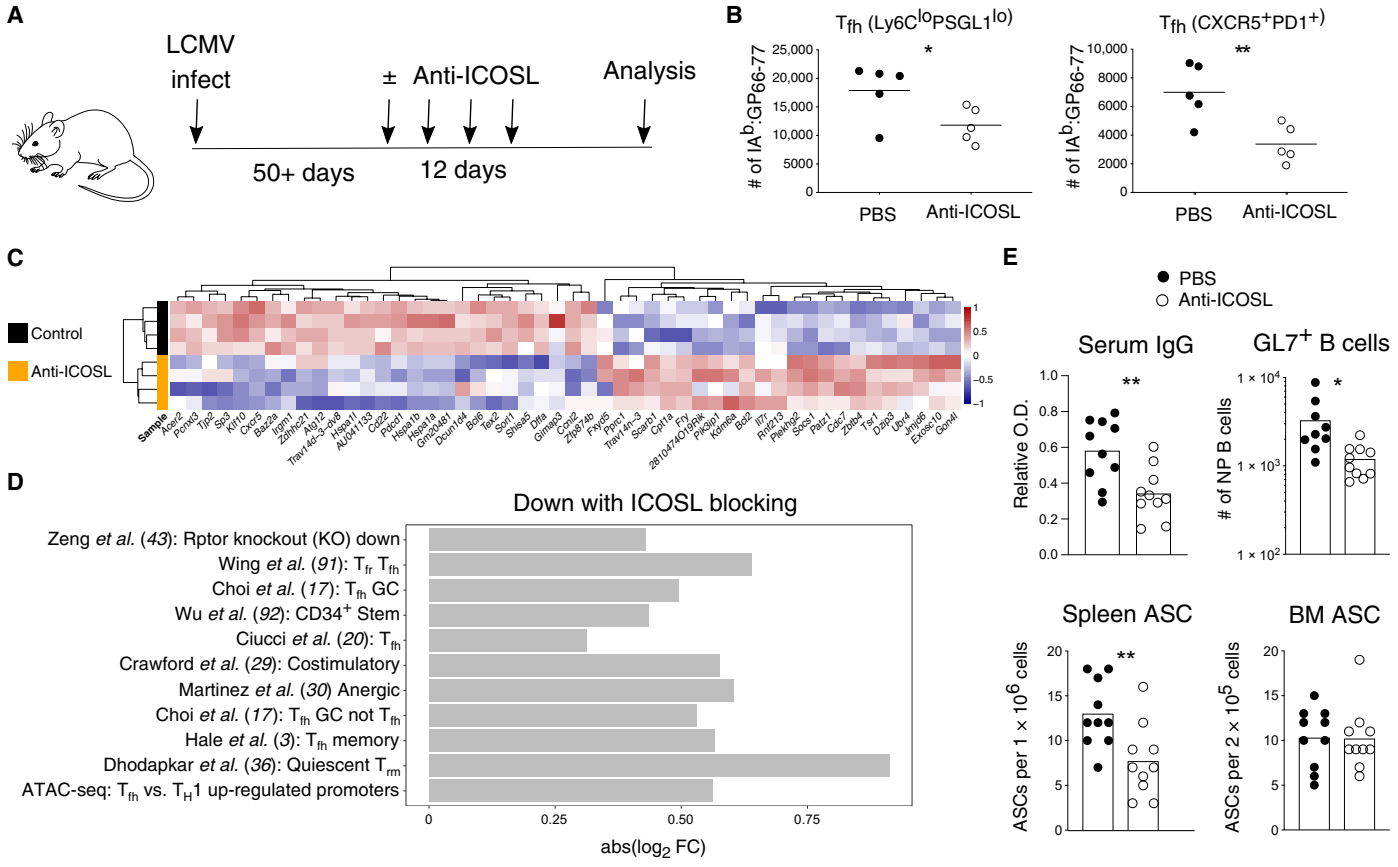

Fig. 7. ICOS signaling maintains T_{fh} cell identity. (**A**) Mice infected with LCMV followed by anti-ICOSL treatment at late time points after infection. LCMV-specific $CD4^+$ T and B cells analyzed after 12 days of treatment. (**B**) Cell numbers of GP66-specific long-lived T_{fh} cells in treated mice using different gating strategies. (**C**) Scaled, centered expression of 20 most significant differentially expressed transcripts in long-lived T_{fh} cells between control and anti-ICOSL–treated mice. (**D**) Most significantly down-regulated gene signatures with anti-ICOSL–blocking (false discovery rate < 0.2) (*3*, *17*, *20*, *29*, *30*, *36*, *43*, *91*, *92*). (**E**) NP-specific IgG serum titer [far left, optical density (O.D.) measured in 1:8100 dilution], numbers of NP-specific $GL7^+$ B cells (left), and NP-specific antibody-secreting cells (ASC) from the spleen (right) and bone marrow (far right). Data represent one of $N = 2$ independent experiments with $n = 5$ mice per group (B). Data summarize $N = 2$ independent experiments with $n = 9$ to 10 mice per group, and bars indicate the mean (E). Unpaired two-tailed Student's *t* test was performed for (B) and (E) with $^*P < 0.05$ and $^{**}P < 0.01$.

and stem cell–associated sets in treated samples compared with controls (Fig. 7D). These data emphasize the importance of ICOS signals in maintaining long-lived T_{fh} identity.

At late time points after LCMV infection, antibody titers are maintained by plasma cells present in the bone marrow (*66*, *67*). However, up to 1 year after infection, about 20% of the total plasma cell compartment is found in the spleen, with an estimated half-life of 172 days (*68*, *69*). The contribution of long-lived T_{fh} cells to plasma cell maintenance or antibody titers has not been considered due to the previous inability to detect T_{fh} cells at late time points. To assess whether late ICOS blockade and subsequent decline of the long-lived T_{fh} cell compartment affect late phase humoral responses, we measured LCMV-specific antibody titers in the serum of treated and control mice at day >60. Here, we observed an almost twofold decrease in NP-specific immunoglobulin G (IgG) antibody titers with ICOS blockade (Fig. 7E). To determine whether the decline in antibody titers correlated with fewer plasma cells in the bone marrow or spleen, we measured the number of NP-specific plasma cells by ELISpot. Here, we observed that anti-ICOSL treatment correlated with a twofold decrease in the number of splenic plasma cells, with no impact on the number of bone marrow plasma cells (Fig. 7E). Assuming that ICOS blocking is 100% efficient and that circulating IgG has a half-life of about 8 days, these data reveal a sizeable and ongoing contribution of splenic plasma cells to antibody maintenance at this time point (fig. S7C). Because both anti-ICOSL and 2-DG/rapamycin treatments result in decreased numbers of long-lived T_{fh} cells, we tested whether antibody titers decrease after 2-DG/rapamycin treatment. 2-DG/rapamycin did not affect circulating antibody titers (fig. S7D). One possible explanation is that the low dose of rapamycin used primarily inhibits mTORC1 signaling, whereas ICOS signals are additionally mediated by mTORC2 (*43*). In support of this idea, anti-ICOSL treatment decreased the expression of mTORC2 target proteins IL-7R and CCR7 on T_{fh} cells, whereas T_{fh} cells from 2-DG/rapamycin and control mice maintained higher levels of these proteins (fig. S7E).

To further assess humoral responses, we counted germinal centers (GCs) at late time points after LCMV infection using immunohistochemistry. Although GCs were clearly detected at day 15 after infection, their number at day 54 was comparable with the number in uninfected mice of a similar age (fig. S7F). We next used an NP tetramer to determine whether virus-specific B cells were affected by ICOSL blockade (*70*). Numbers of IgD, IgM, and isotype-switched

immunoglobulin (swIg) memory B cells were unaffected, but there was a significant decrease in the number and proportion of GL7$^+$ B cells (fig. S7G and Fig. 7E). These cells did not express Fas, a marker normally associated with active GC B cells and that, when absent, has been reported to preferentially support plasma cell differentiation (fig. S7H) (*71*). GL7$^+$Fas$^-$ B cells were also negative for CD38 and CD138, distinguishing them from B memory or plasmablasts (fig. S7I). In addition, most of these cells were double negative for IgM and IgD and expressed both CD73 and CD80, markers associated with prior participation in a GC reaction (fig. S7J) (*72*). Together, these data demonstrate an essential role for ICOS signaling in maintaining the long-lived T_{fh} compartment and plasma cell survival in the spleen.

DISCUSSION

In this study, we determined that the CD4$^+$ memory compartment contains an abundant and highly persistent population of long-lived T_{fh} cells with broad recall capacity after secondary challenge. The presence of T_{fh} memory has been controversial. Although cells with T_{fh} cell markers have been identified in the memory phase after infection, it is unclear whether they represent an ongoing immune response, whether they are "rested down" T_{fh} memory cells, or whether they are a distinct population of self-renewing T_{cm} cells with T_{fh}-like characteristics (*73*). Our data demonstrating the extreme susceptibility of T_{fh} cells to death during isolation from the tissue shed light on the previous difficulty in discriminating these possibilities. Earlier studies reporting that T_{fh} memory cells have a muted phenotype, with decreased or absent expression of CXCR5 and PD1, respectively, were conducted with monoclonal populations of TCR transgenic cells transferred in high numbers that may not accurately reflect the breadth in differentiation of a polyclonal repertoire (*3*, *12*, *21*). Consistent with the idea that T cell differentiation can be partially informed by TCR signals, a cell-intrinsic bias for various TCR transgenic strains has previously been reported (*21*). In addition to confirming more limited long-lived T_{fh} differentiation by two distinct TCR transgenic strains, we show that treatment with NICD protector rescues polyclonal T_{fh} cells at all time points, preserving their phenotype and exposing their metabolic fitness and unexpected longevity. In contrast, T_{cm} cells, generally considered to be self-renewing and multipotent, are largely absent at the latest time points after infection. Previous studies have suggested the existence of memory cells with a hybrid T_{fh}/T_{cm} phenotype, namely, dual expression of CXCR5 and CCR7 (*6*, *12*, *20*). Our data on NICD-susceptible samples confirm a population of CXCR5$^+$CCR7$^+$ memory cells that likely represents cells on the border of transition from T_{fh} to T_{cm}/T_H1. However, the addition of NICD protector reveals that these transitional cells constitute a small minority of the total CD4$^+$ population at memory time points. When cells are protected from NICD, CCR7 and CXCR5 are negatively correlated. In addition, we show that CXCR5 as a marker to define the T_{fh} memory compartment is complicated by the expression of this protein in non-T_{fh} subsets. Using scRNA-seq and flow cytometry, we demonstrate that long-lived T_{fh} and T_{cm} populations are more clearly discriminated by *Izumo1r*/FR4 expression.

We further show that long-lived T_{fh} cells require ongoing ICOS signals and mTOR/glycolysis for their survival. These observations suggest that maintenance of long-lived T_{fh} cells is an active process. In the absence of ICOS signaling, long-lived T_{fh} cells may re-localize and acquire T_H1 memory cell characteristics, as previously reported for T_{fh} effector cells (*74*). This idea is consistent with our experiments demonstrating the inherent plasticity of long-lived T_{fh} cells after transfer, although under unperturbed conditions, ICOS-mediated retention of long-lived T_{fh} cells in proximity with B cells may limit their secondary effector potential. These data are also in line with a recent study showing the importance of ICOS signals for the maintenance of lung-resident CD4$^+$ T cells induced by tuberculosis infection (*75*). Our scRNA-seq data reveal transcriptional similarity between long-lived T_{fh} and T_{rm} cells, both recognized as noncirculating subsets. As both residency and mTOR gene expression signatures are reduced in long-lived T_{fh} cells after ICOS blockade, it will be interesting to determine whether ICOS and mTOR signals are required to sustain T_{rm} cells after acute infection.

The constitutive glycolytic phenotype we observed in long-lived T_{fh} cells occurs together with high expression of TCF1 and CD27, both associated with self-renewal and plasticity. These data are notably in contrast to many studies showing a positive correlation between catabolic metabolism and stem-like features. In general, effector T cell differentiation is associated with a more glycolytic metabolism, whereas memory T cells exhibit a shift toward oxidative metabolism (*76*). Previous studies have shown that inhibition of mTOR signals promotes the generation of both CD4$^+$ and CD8$^+$ memory T cells (*77*–*79*). mTOR activation was also recently shown to mediate the differentiation of metabolically quiescent, TCF1-positive TH17 cells into inflammatory T_H1 effectors (*50*). On the other hand, CD4$^+$ memory T cells require Notch-dependent glucose uptake for survival, and CD8$^+$ T cells with enforced glycolytic metabolism are still able to generate memory T cells with robust recall capacity, albeit with a bias toward the CD62L^{lo} T_{em} phenotype (*80*, *81*). Similarly, human CD4$^+$ T_{em} cells have an increased glycolytic reserve and depend on glycolysis to maintain mitochondrial membrane potential, regulating both survival and recall potential (*82*). Together, our findings suggest that engagement of a specific metabolic pathway does not universally underlie the differentiation of memory T cells and that different types of memory T cells may preferentially use metabolic pathways that are tuned to a particular immune context (e.g., availability of cytokines, nutrients, antigen, etc.).

Last, our data reveal an unexpected role for T_{fh} cells in supporting splenic plasma cells and systemic antibody titers at time points when the immune response has supposedly died down. Because of the apparent absence of long-lived T_{fh} cells without NICD protector, a role for T_{fh} cells was not previously considered. One possibility is that persistent antigen fuels the continuous differentiation of memory B cells into plasma cells (*83*). The observation of decreased NP-specific GL7$^+$ B cells after ICOS blockade is compatible with this idea, although GL7$^+$ B cells isolated at these late time points did not express Fas and therefore have an unusual phenotype. It is possible that GL7$^+$Fas$^-$ cells received fewer costimulatory signals (e.g., CD40 cross-linking), which would otherwise induce Fas expression, or that these cells are recent GC emigrants, which may later up-regulate CD38 and transition into the memory B cell compartment. We also did not see a change in NP-specific plasmablast numbers, although we cannot exclude effects of technical limitations. In addition, abundant T_{fh} cells were detected 400+ days after infection, which points to either astonishingly long antigen persistence or an alternative explanation. Another possibility is that ICOS blocking interferes with the structural organization of the spleen and/or plasma cell niche. Plasma cell survival depends on the availability of soluble factors, such as IL-6, IL-21, and B-cell activating factor (BAFF), all of which

can be produced by T_{fh} cells (*84*). Both $CD4^+$ T cells and BAFF were recently identified as key factors supporting the survival of splenic plasma cells, but the nature of $CD4^+$-derived signals was not reported (*85*). One way to discriminate the function of long-lived T_{fh} cells will be to understand where these cells are localized. During the effector phase, T_{fh} cells localize to B cell follicles by interacting with ICOSL expressed by bystander B cells (*86*). If long-lived T_{fh} cells support the conversion of memory B cells into plasma cells, we would expect this colocalization to continue at late time points after infection. On the other hand, if long-lived T_{fh} cells directly provide survival signals to plasma cells, they may be localized in or near the red pulp. In this scenario, long-lived T_{fh} cell interactions with $CD11c^+$ ICOSL- expressing antigen presenting cells would be impaired by ICOSL blockade, leading to a loss of T_{fh} cells (*87*).

The observation that ICOS blocking reduces NP-specific IgG titers roughly twofold is unexpected if splenic plasma cells make up only 20% of the total plasma cell pool, as has been previously estimated (*67*). One possibility is that this original calculation underestimates the number of splenic plasma cells at this time point; alternatively, antibody output from splenic plasma cells may be higher compared with bone marrow cells. With respect to the first possibility, the original estimate of 20% is based on the number of plasma cells in the mouse femur, under the assumption that all bone marrow compartments have equivalent plasma cell activity. However, a recent study in macaques demonstrated that plasma cells preferentially accumulate in the femur compared with other bones, suggesting that the current conversion factor for mice—based solely on counts from the femur—may overestimate the total number of bone marrow splenic cells (*88*).

In summary, our data establish long-lived T_{fh} cells as an attractive target for vaccination. The question remains, however, as to whether these cells can be termed memory cells. This debate assumes a classical definition of memory, hinging on questions of antigen availability and dependence. Although our experiments demonstrate that a large proportion of polyclonal T_{fh} cells can survive in the absence of antigen, their recovery is highest after transfer into infection-matched recipients. Nevertheless, at day 400+ after infection, when residual antigen is unlikely to play a major role, T_{fh} cells make up a substantial proportion of the antigen-specific compartment. When identified by the absence of CCR7 and CD62L, long-lived T_{fh} cells can be considered a T_{em} subset. $CD4^+$ T_{em} cells were recently shown to be generated in response to a universal influenza vaccination and to correlate with accelerated and improved cellular and humoral secondary responses after challenge (*89*). In contrast, the unanticipated scarcity of T_{cm} cells at late time points that we report here combined with their more limited recall potential indicates that vaccines targeting T_{cm} may not offer optimal long-term protection.

MATERIALS AND METHODS

Study design

The aim of this study was to understand the longevity and differentiation potential of distinct $CD4^+$ memory T cell subsets. We used the murine LCMV infection model and major histocompatibility complex II tetramers to identify polyclonal antigen-specific $CD4^+$ memory T cells. Detailed descriptions of experimental parameters (sample sizes, number of experimental replicates, and statistical analysis) can be found below or in figure legends. Infected mice were randomly assigned to treatment versus control groups. Analysis of the experimental data was conducted in an unblinded manner.

Mice

Mice were bred and housed under specific pathogen-free conditions at the University Hospital of Basel according to the animal protection law in Switzerland. For all experiments, male or female sex-matched mice that were at least 6 weeks old at the time point of infection were used. The following mouse strains were used: C57BL/6 CD45.2, C57BL/6 CD45.1, Nur77 green fluorescent protein (GFP), c-myc GFP (provided by T. Schroeder, Department of Biosystems Science and Engineering, Switzerland), T-bet ZsGreen (provided by J. Zhu, National Institutes of Health, USA), $P2X7R^{-/-}$ (provided by F. Grassi, Institute for Research in Biomedicine, Switzerland), SMARTA, and NIP (S. Crotty, La Jolla Institute for Allergy and Immunology, USA).

NICD protector

Mice were intravenously injected with 25 μg of commercial (BioLegend, no. 149802) or 12.5 μg of homemade ARTC2.2-blocking nanobody s+16 (NICD protector) 15 min before organ harvest. NICD protector was used in every experiment (including adoptive transfers) except for when the goal was to compare NICD protector treatment to no treatment (Fig. 1, A and C, and figs. S1, C to E and G, and S3, I to K).

Statistical analysis

For statistical analysis, the tests that were used are specified in each figure legend. In time course experiments, statistical analysis was performed for each individual time point. Error bars show SD centered on the mean unless otherwise indicated. Data were analyzed with GraphPad Prism software (version 7 or 8). $*P < 0.05$, $**P < 0.01$, $***P < 0.001$, $****P < 0.0001$. ns, not significant.

SUPPLEMENTARY MATERIALS

immunology.sciencemag.org/cgi/content/full/5/45/eaay5552/DC1

Methods

Fig. S1. T_{fh} cells are susceptible to death during isolation.

Fig. S2. FR4 discriminates long-lived T_{fh} from transcriptionally distinct T_{cm}.

Fig. S3. Long-lived T_{fh} cells are constitutively glycolytic.

Fig. S4. Antigen is not required for the survival of long-lived T_{fh} cells.

Fig. S5. T_{fh} cells generate multiple cell fates upon recall.

Fig. S6. Epigenetic regulation of long-lived T_{fh} cells.

Fig. S7. ICOS signaling maintains T_{fh} cell identity at late time points.

Fig. S8. Normalization of ATAC-seq data.

Table S1. Raw data file (Excel spreadsheet).

References (*93*–*105*)

View/request a protocol for this paper from *Bio-protocol*.

REFERENCES AND NOTES

1. R. Ahmed, D. Gray, Immunological memory and protective immunity: Understanding their relation. *Science* **272**, 54–60 (1996).
2. F. Sallusto, J. Geginat, A. Lanzavecchia, Central memory and effector memory T cell subsets: Function, generation, and maintenance. *Annu. Rev. Immunol.* **22**, 745–763 (2004).
3. J. S. Hale, B. Youngblood, D. R. Latner, A.-U.-R. Mohammed, L. Ye, R. S. Akondy, T. Wu, S. S. Iyer, R. Ahmed, Distinct memory $CD4^+$ T cells with commitment to T follicular helper- and T helper 1-cell lineages are generated after acute viral infection. *Immunity* **38**, 805–817 (2013).
4. M. K. MacLeod, A. David, A. S. McKee, F. Crawford, J. W. Kappler, P. Marrack, Memory CD4 T cells that express CXCR5 provide accelerated help to B cells. *J. Immunol.* **186**, 2889–2896 (2011).
5. K. Luthje, A. Kallies, Y. Shimohakamada, G. T. Belz, A. Light, D. M. Tarlinton, S. L. Nutt, The development and fate of follicular helper T cells defined by an IL-21 reporter mouse. *Nat. Immunol.* **13**, 491–498 (2012).
6. M. Pepper, A. J. Pagán, B. Z. Igyártó, J. J. Taylor, M. K. Jenkins, Opposing signals from the Bcl6 transcription factor and the interleukin-2 receptor generate T helper 1 central and effector memory cells. *Immunity* **35**, 583–595 (2011).

7. A. Asrir, M. Aloulou, M. Gador, C. Pérals, N. Fazilleau, Interconnected subsets of memory follicular helper T cells have different effector functions. *Nat. Commun.* **8**, 847 (2017).
8. S. E. Bentebibel, S. Lopez, G. Obermoser, N. Schmitt, C. Mueller, C. Harrod, E. Flano, A. Mejias, R. A. Albrecht, D. Blankenship, H. Xu, V. Pascual, J. Banchereau, A. Garcia-Sastre, A. K. Palucka, O. Ramilo, H. Ueno, Induction of $ICOS^+CXCR3^+CXCR5^+$ T_H cells correlates with antibody responses to influenza vaccination. *Sci. Transl. Med.* **5**, 176ra32 (2013).
9. S. Crotty, R. Ahmed, *Immune Memory and Vaccines: Great Debates* (Cold Spring Harbor perspectives in biology, Cold Spring Harbor Laboratory Press, Cold Spring Harbor, New York, 2018), pp. ix, 418 pages.
10. D. L. Hill, W. Pierson, D. J. Bolland, C. Mkindi, E. J. Carr, J. Wang, S. Houard, S. W. Wingett, R. Audran, E. F. Wallin, S. A. Jongo, K. Kamaka, M. Zand, F. Spertini, C. Daubenberger, A. E. Corcoran, M. A. Linterman, The adjuvant GLA-SE promotes human Tfh cell expansion and emergence of public TCRβ clonotypes. *J. Exp. Med.* **216**, 1857–1873 (2019).
11. S. Keck, M. Schmaler, S. Ganter, L. Wyss, S. Oberle, E. S. Huseby, D. Zehn, C. G. King, Antigen affinity and antigen dose exert distinct influences on CD4 T-cell differentiation. *Proc. Natl. Acad. Sci. U.S.A.* **111**, 14852–14857 (2014).
12. H. D. Marshall, A. Chandele, Y. W. Jung, H. Meng, A. C. Poholek, I. A. Parish, R. Rutishauser, W. Cui, S. H. Kleinstein, J. Craft, S. M. Kaech, Differential expression of Ly6C and T-bet distinguish effector and memory T_H1 $CD4^+$ cell properties during viral infection. *Immunity* **35**, 633–646 (2011).
13. D. Homann, L. Teyton, M. B. A. Oldstone, Differential regulation of antiviral T-cell immunity results in stable $CD8^+$ but declining $CD4^+$ T-cell memory. *Nat. Med.* **7**, 913–919 (2001).
14. M. A. Williams, E. V. Ravkov, M. J. Bevan, Rapid culling of the $CD4^+$ T cell repertoire in the transition from effector to memory. *Immunity* **28**, 533–545 (2008).
15. H. D. Marshall, J. P. Ray, B. J. Laidlaw, N. Zhang, D. Gawande, M. M. Staron, J. Craft, S. M. Kaech, The transforming growth factor beta signaling pathway is critical for the formation of CD4 T follicular helper cells and isotype-switched antibody responses in the lung mucosa. *eLife* **4**, e04851 (2015).
16. Y. Tian, M. Babor, J. Lane, V. Schulten, V. S. Patil, G. Seumois, S. L. Rosales, Z. Fu, G. Picarda, J. Burel, J. Zapardiel-Gonzalo, R. N. Tennekoon, A. D. De Silva, S. Premawansa, G. Premawansa, A. Wijewickrama, J. A. Greenbaum, P. Vijayanand, D. Weiskopf, A. Sette, B. Peters, Unique phenotypes and clonal expansions of human CD4 effector memory T cells re-expressing CD45RA. *Nat. Commun.* **8**, 1473 (2017).
17. Y. S. Choi, J. A. Gullicksrud, S. Xing, Z. Zeng, Q. Shan, F. Li, P. E. Love, W. Peng, H.-H. Xue, S. Crotty, LEF-1 and TCF-1 orchestrate T_{FH} differentiation by regulating differentiation circuits upstream of the transcriptional repressor Bcl6. *Nat. Immunol.* **16**, 980–990 (2015).
18. A. M. Siegel, J. Heimall, A. F. Freeman, A. P. Hsu, E. Brittain, J. M. Brenchley, D. C. Douek, G. H. Fahle, J. I. Cohen, S. M. Holland, J. D. Milner, A critical role for STAT3 transcription factor signaling in the development and maintenance of human T cell memory. *Immunity* **35**, 806–818 (2011).
19. C. S. Ma, D. T. Avery, A. Chan, M. Batten, J. Bustamante, S. Boisson-Dupuis, P. D. Arkwright, A. Y. Kreins, D. Averbuch, D. Engelhard, K. Magdorf, S. S. Kilic, Y. Minegishi, S. Nonoyama, M. A. French, S. Choo, J. M. Smart, J. Peake, M. Wong, P. Gray, M. C. Cook, D. A. Fulcher, J.-L. Casanova, E. K. Deenick, S. G. Tangye, Functional STAT3 deficiency compromises the generation of human T follicular helper cells. *Blood* **119**, 3997–4008 (2012).
20. T. Ciucci, M. S. Vacchio, Y. Gao, F. Tomassoni Ardori, J. Candia, M. Mehta, Y. Zhao, B. Tran, M. Pepper, L. Tessarollo, D. B. McGavern, R. Bosselut, The emergence and functional fitness of memory $CD4^+$ T cells require the transcription factor Thpok. *Immunity* **50**, 91–105.e4 (2019).
21. N. J. Tubo, A. J. Pagán, J. J. Taylor, R. W. Nelson, J. L. Linehan, J. M. Ertelt, E. S. Huseby, S. S. Way, M. K. Jenkins, Single naive $CD4^+$ T cells from a diverse repertoire produce different effector cell types during infection. *Cell* **153**, 785–796 (2013).
22. Y. S. Choi, J. A. Yang, I. Yusuf, R. J. Johnston, J. Greenbaum, B. Peters, S. Crotty, Bcl6 expressing follicular helper CD4 T cells are fate committed early and have the capacity to form memory. *J. Immunol.* **190**, 4014–4026 (2013).
23. S. S. Iyer, D. R. Latner, M. J. Zilliox, M. M. Causland, R. S. Akondy, P. Penaloza-MacMaster, J. S. Hale, L. Ye, A.-U.-R. Mohammed, T. Yamaguchi, S. Sakaguchi, R. R. Amara, R. Ahmed, Identification of novel markers for mouse $CD4^+$ T follicular helper cells. *Eur. J. Immunol.* **43**, 3219–3232 (2013).
24. M. Proietti, V. Cornacchione, T. Rezzonico Jost, A. Romagnani, C. E. Faliti, L. Perruzza, R. Rigoni, E. Radaelli, F. Caprioli, S. Preziuso, B. Brannetti, M. Thelen, K. D. McCoy, E. Slack, E. Traggiai, F. Grassi, ATP-gated ionotropic P2X7 receptor controls follicular T helper cell numbers in Peyer's patches to promote host-microbiota mutualism. *Immunity* **41**, 789–801 (2014).
25. F. Aswad, H. Kawamura, G. Dennert, High sensitivity of $CD4^+CD25^+$ regulatory T cells to extracellular metabolites nicotinamide adenine dinucleotide and ATP: A role for $P2X_7$ receptors. *J. Immunol.* **175**, 3075–3083 (2005).
26. D. Fernandez-Ruiz, W. Y. Ng, L. E. Holz, J. Z. Ma, A. Zaid, Y. C. Wong, L. S. Lau, V. Mollard, A. Cozijnsen, N. Collins, J. Li, G. M. Davey, Y. Kato, S. Devi, R. Skandari, M. Pauley, J. H. Manton, D. I. Godfrey, A. Braun, S. S. Tay, P. S. Tan, D. G. Bowen, F. Koch-Nolte, B. Rissiek, F. R. Carbone, B. S. Crabb, M. Lahoud, I. A. Cockburn, S. N. Mueller, P. Bertolino, G. I. McFadden, I. Caminschi, W. R. Heath, Liver-resident memory $CD8^+$ T cells form a front-line defense against malaria liver-stage infection. *Immunity* **45**, 889–902 (2016).
27. S. Hubert, B. Rissiek, K. Klages, J. Huehn, T. Sparwasser, F. Haag, F. Koch-Nolte, O. Boyer, M. Seman, S. Adriouch, Extracellular NAD^+ shapes the $Foxp3^+$ regulatory T cell compartment through the ART2–P2X7 pathway. *J. Exp. Med.* **207**, 2561–2568 (2010).
28. H. Borges da Silva, H. Wang, L. J. Qian, K. A. Hogquist, S. C. Jameson, ARTC2.2/P2RX7 signaling during cell isolation distorts function and quantification of tissue-resident $CD8^+$ T cell and invariant NKT subsets. *J. Immunol.* **202**, 2153–2163 (2019).
29. A. Crawford, J. M. Angelosanto, C. Kao, T. A. Doering, P. M. Odorizzi, B. E. Barnett, E. J. Wherry, Molecular and transcriptional basis of $CD4^+$ T cell dysfunction during chronic infection. *Immunity* **40**, 289–302 (2014).
30. G. J. Martinez, R. M. Pereira, T. Äijö, E. Y. Kim, F. Marangoni, M. E. Pipkin, S. Togher, V. Heissmeyer, Y. C. Zhang, S. Crotty, E. D. Lamperti, K. M. Ansel, T. R. Mempel, H. Lähdesmäki, P. G. Hogan, A. Rao, The transcription factor NFAT promotes exhaustion of activated $CD8^+$ T cells. *Immunity* **42**, 265–278 (2015).
31. L. A. Kalekar, S. E. Schmiel, S. L. Nandiwada, W. Y. Lam, L. O. Barsness, N. Zhang, G. L. Stritesky, D. Malhotra, K. E. Pauken, J. L. Linehan, M. G. O'Sullivan, B. T. Fife, K. A. Hogquist, M. K. Jenkins, D. L. Mueller, $CD4^+$ T cell anergy prevents autoimmunity and generates regulatory T cell precursors. *Nat. Immunol.* **17**, 304–314 (2016).
32. T. Yamaguchi, K. Hirota, K. Nagahama, K. Ohkawa, T. Takahashi, T. Nomura, S. Sakaguchi, Control of immune responses by antigen-specific regulatory T cells expressing the folate receptor. *Immunity* **27**, 145–159 (2007).
33. M. M. McCausland, S. Crotty, Quantitative PCR technique for detecting lymphocytic choriomeningitis virus in vivo. *J. Virol. Methods* **147**, 167–176 (2008).
34. L. K. Mackay, M. Minnich, N. A. M. Kragten, Y. Liao, B. Nota, C. Seillet, A. Zaid, K. Man, S. Preston, D. Freestone, A. Braun, E. Wynne-Jones, F. M. Behr, R. Stark, D. G. Pellicci, D. I. Godfrey, G. T. Belz, M. Pellegrini, T. Gebhardt, M. Busslinger, W. Shi, F. R. Carbone, R. A. W. van Lier, A. Kallies, K. P. J. M. van Gisbergen, Hobit and Blimp1 instruct a universal transcriptional program of tissue residency in lymphocytes. *Science* **352**, 459–463 (2016).
35. L. K. Mackay, A. Rahimpour, J. Z. Ma, N. Collins, A. T. Stock, M.-L. Hafon, J. Vega-Ramos, P. Lauzurica, S. N. Mueller, T. Stefanovic, D. C. Tscharke, W. R. Heath, M. Inouye, F. R. Carbone, T. Gebhardt, The developmental pathway for $CD103^+CD8^+$ tissue-resident memory T cells of skin. *Nat. Immunol.* **14**, 1294–1301 (2013).
36. C. S. Boddupalli, S. Nair, S. M. Gray, H. N. Nowyhed, R. Verma, J. A. Gibson, C. Abraham, D. Narayan, J. Vasquez, C. C. Hedrick, R. A. Flavell, K. M. Dhodapkar, S. M. Kaech, M. V. Dhodapkar, ABC transporters and NR4A1 identify a quiescent subset of tissue-resident memory T cells. *J. Clin. Invest.* **126**, 3905–3916 (2016).
37. S. H. Cho, A. L. Raybuck, J. Blagih, E. Kemboi, V. H. Haase, R. G. Jones, M. R. Boothby, Hypoxia-inducible factors in $CD4^+$ T cells promote metabolism, switch cytokine secretion, and T cell help in humoral immunity. *Proc. Natl. Acad. Sci. U.S.A.* **116**, 8975–8984 (2019).
38. Y. Zhu, Y. Zhao, L. Zou, D. Zhang, D. Aki, Y.-C. Liu, The E3 ligase VHL promotes follicular helper T cell differentiation via glycolytic-epigenetic control. *J. Exp. Med.* **216**, 1664–1681 (2019).
39. P. Hombrink, C. Helbig, R. A. Backer, B. Piet, A. E. Oja, R. Stark, G. Brasser, A. Jongejan, R. E. Jonkers, B. Nota, O. Basak, H. C. Clevers, P. D. Moerland, D. Amsen, R. A. W. van Lier, Programs for the persistence, vigilance and control of human $CD8^+$ lung-resident memory T cells. *Nat. Immunol.* **17**, 1467–1478 (2016).
40. S. Bekkering, R. J. W. Arts, B. Novakovic, I. Kourtzelis, C. D. C. C. van der Heijden, Y. Li, C. D. Popa, R. ter Horst, J. van Tuijl, R. T. Netea-Maier, F. L. van de Veerdonk, T. Chavakis, L. A. B. Joosten, J. W. M. van der Meer, H. Stunnenberg, N. P. Riksen, M. G. Netea, Metabolic induction of trained immunity through the mevalonate pathway. *Cell* **172**, 135–146.e9 (2018).
41. S.-C. Cheng, J. Quintin, R. A. Cramer, K. M. Shepardson, S. Saeed, V. Kumar, E. J. Giamarellos-Bourboulis, J. H. A. Martens, N. A. Rao, A. Aghajanirefah, G. R. Manjeri, Y. Li, D. C. Ifrim, R. J. W. Arts, B. M. J. W. van der Veer, P. M. T. Deen, C. Logie, L. A. O'Neill, P. Willems, F. L. van de Veerdonk, J. W. M. van der Meer, A. Ng, L. A. B. Joosten, C. Wijmenga, H. G. Stunnenberg, R. J. Xavier, M. G. Netea, mTOR- and HIF-1α–mediated aerobic glycolysis as metabolic basis for trained immunity. *Science* **345**, 1250684 (2014).
42. S. Saeed, J. Quintin, H. H. D. Kerstens, N. A. Rao, A. Aghajanirefah, F. Matarese, S.-C. Cheng, J. Ratter, K. Berentsen, M. A. van der Ent, N. Sharifi, E. M. Janssen-Megens, M. T. Huurne, A. Mandoli, T. van Schaik, A. Ng, F. Burden, K. Downes, M. Frontini, V. Kumar, E. J. Giamarellos-Bourboulis, W. H. Ouwehand, J. W. M. van der Meer, L. A. B. Joosten, C. Wijmenga, J. H. A. Martens, R. J. Xavier, C. Logie, M. G. Netea, H. G. Stunnenberg, Epigenetic programming of monocyte-to-macrophage differentiation and trained innate immunity. *Science* **345**, 1251086 (2014).
43. H. Zeng, S. Cohen, C. Guy, S. Shrestha, G. Neale, S. A. Brown, C. Cloer, R. J. Kishton, X. Gao, B. Youngblood, M. Do, M. O. Li, J. W. Locasale, J. C. Rathmell, H. Chi, mTORC1 and mTORC2 kinase signaling and glucose metabolism drive follicular helper T cell differentiation. *Immunity* **45**, 540–554 (2016).
44. D. K. Finlay, E. Rosenzweig, L. V. Sinclair, C. Feijoo-Carnero, J. L. Hukelmann, J. Rolf, A. A. Panteleyev, K. Okkenhaug, D. A. Cantrell, PDK1 regulation of mTOR and

hypoxia-inducible factor 1 integrate metabolism and migration of $CD8^+$ T cells. *J. Exp. Med.* **209**, 2441–2453 (2012).
45. A. Lissina, K. Ladell, A. Skowera, M. Clement, E. Edwards, R. Seggewiss, H. A. van den Berg, E. Gostick, K. Gallagher, E. Jones, J. J. Melenhorst, A. J. Godkin, M. Peakman, D. A. Price, A. K. Sewell, L. Wooldridge, Protein kinase inhibitors substantially improve the physical detection of T-cells with peptide-MHC tetramers. *J. Immunol. Methods* **340**, 11–24 (2009).
46. J. P. Ray, M. M. Staron, J. A. Shyer, P.-C. Ho, H. D. Marshall, S. M. Gray, B. J. Laidlaw, K. Araki, R. Ahmed, S. M. Kaech, J. Craft, The interleukin-2-mTORc1 kinase axis defines the signaling, differentiation, and metabolism of T helper 1 and follicular B helper T cells. *Immunity* **43**, 690–702 (2015).
47. H. Borges da Silva, L. K. Beura, H. Wang, E. A. Hanse, R. Gore, M. C. Scott, D. A. Walsh, K. E. Block, R. Fonseca, Y. Yan, K. L. Hippen, B. R. Blazar, D. Masopust, A. Kelekar, L. Vulchanova, K. A. Hogquist, S. C. Jameson, The purinergic receptor P2RX7 directs metabolic fitness of long-lived memory $CD8^+$ T cells. *Nature* **559**, 264–268 (2018).
48. J. Hendriks, L. A. Gravestein, K. Tesselaar, R. A. W. van Lier, T. N. M. Schumacher, J. Borst, CD27 is required for generation and long-term maintenance of T cell immunity. *Nat. Immunol.* **1**, 433–440 (2000).
49. M. Pepper, J. L. Linehan, A. J. Pagán, T. Zell, T. Dileepan, P. P. Cleary, M. K. Jenkins, Different routes of bacterial infection induce long-lived T_H1 memory cells and short-lived T_H17 cells. *Nat. Immunol.* **11**, 83–89 (2010).
50. P. W. F. Karmaus, X. Chen, S. A. Lim, A. A. Herrada, T.-L. M. Nguyen, B. Xu, Y. Dhungana, S. Rankin, W. Chen, C. Rosencrance, K. Yang, Y. Fan, Y. Cheng, J. Easton, G. Neale, P. Vogel, H. Chi, Metabolic heterogeneity underlies reciprocal fates of T_H17 cell stemness and plasticity. *Nature* **565**, 101–105 (2019).
51. H. Moon, H.-Y. Na, K. H. Chong, T. J. Kim, P2X7 receptor-dependent ATP-induced shedding of CD27 in mouse lymphocytes. *Immunol. Lett.* **102**, 98–105 (2006).
52. P. Muranski, Z. A. Borman, S. P. Kerkar, C. A. Klebanoff, Y. Ji, L. Sanchez-Perez, M. Sukumar, R. N. Reger, Z. Yu, S. J. Kern, R. Roychoudhuri, G. A. Ferreyra, W. Shen, S. K. Durum, L. Feigenbaum, D. C. Palmer, P. A. Antony, C. C. Chan, A. Laurence, R. L. Danner, L. Gattinoni, N. P. Restifo, Th17 cells are long lived and retain a stem cell-like molecular signature. *Immunity* **35**, 972–985 (2011).
53. C. Trapnell, D. Cacchiarelli, J. Grimsby, P. Pokharel, S. Li, M. Morse, N. J. Lennon, K. J. Livak, T. S. Mikkelsen, J. L. Rinn, The dynamics and regulators of cell fate decisions are revealed by pseudotemporal ordering of single cells. *Nat. Biotechnol.* **32**, 381–386 (2014).
54. J. D. Buenrostro, P. G. Giresi, L. C. Zaba, H. Y. Chang, W. J. Greenleaf, Transposition of native chromatin for fast and sensitive epigenomic profiling of open chromatin, DNA-binding proteins and nucleosome position. *Nat. Methods* **10**, 1213–1218 (2013).
55. P. Durek, K. Nordström, G. Gasparoni, A. Salhab, C. Kressler, M. de Almeida, K. Bassler, T. Ulas, F. Schmidt, J. Xiong, P. Glažar, F. Klironomos, A. Sinha, S. Kinkley, X. Yang, L. Arrigoni, A. D. Amirabad, F. B. Ardakani, L. Feuerbach, O. Gorka, P. Ebert, F. Müller, N. Li, S. Frischbutter, S. Schlickeiser, C. Cendon, S. Fröhler, B. Felder, N. Gasparoni, C. D. Imbusch, B. Hutter, G. Zipprich, Y. Tauchmann, S. Reinke, G. Wassilew, U. Hoffmann, A. S. Richter, L. Sieverling; DEEP Consortium, H. D. Chang, U. Syrbe, U. Kalus, J. Eils, B. Brors, T. Manke, J. Ruland, T. Lengauer, N. Rajewsky, W. Chen, J. Dong, B. Sawitzki, H. R. Chung, P. Rosenstiel, M. H. Schulz, J. L. Schultze, A. Radbruch, J. Walter, A. Hamann, J. K. Polansky, Epigenomic profiling of human $CD4^+$ T cells supports a linear differentiation model and highlights molecular regulators of memory development. *Immunity* **45**, 1148–1161 (2016).
56. D. M. W. Zaiss, W. C. Gause, L. C. Osborne, D. Artis, Emerging functions of amphiregulin in orchestrating immunity, inflammation, and tissue repair. *Immunity* **42**, 216–226 (2015).
57. S. Heinz, C. Benner, N. Spann, E. Bertolino, Y. C. Lin, P. Laslo, J. X. Cheng, C. Murre, H. Singh, C. K. Glass, Simple combinations of lineage-determining transcription factors prime *cis*-regulatory elements required for macrophage and B cell identities. *Mol. Cell* **38**, 576–589 (2010).
58. C. M. Lau, N. M. Adams, C. D. Geary, O.-E. Weizman, M. Rapp, Y. Pritykin, C. S. Leslie, J. C. Sun, Epigenetic control of innate and adaptive immune memory. *Nat. Immunol.* **19**, 963–972 (2018).
59. D. M. Moskowitz, D. W. Zhang, B. Hu, S. L. Saux, R. E. Yanes, Z. Ye, J. D. Buenrostro, C. M. Weyand, W. J. Greenleaf, J. J. Goronzy, Epigenomics of human CD8 T cell differentiation and aging. *Sci. Immunol.* **2**, eaag0192 (2017).
60. I. M. Djuretic, D. Levanon, V. Negreanu, Y. Groner, A. Rao, K. M. Ansel, Transcription factors T-bet and Runx3 cooperate to activate *Ifng* and silence *Il4* in T helper type 1 cells. *Nat. Immunol.* **8**, 145–153 (2007).
61. K. Kohu, H. Ohmori, W. F. Wong, D. Onda, T. Wakoh, S. Kon, M. Yamashita, T. Nakayama, M. Kubo, M. Satake, The Runx3 transcription factor augments T_h1 and down-modulates Th2 phenotypes by interacting with and attenuating GATA3. *J. Immunol.* **183**, 7817–7824 (2009).
62. A. Kramer, J. Green, J. Pollard Jr., S. Tugendreich, Causal analysis approaches in Ingenuity Pathway Analysis. *Bioinformatics* **30**, 523–530 (2014).
63. K. Majchrzak, M. H. Nelson, J. S. Bowers, S. R. Bailey, M. M. Wyatt, J. M. Wrangle, M. P. Rubinstein, J. C. Varela, Z. Li, R. A. Himes, S. S. L. Chan, C. M. Paulos, β-catenin and PI3Kδ inhibition expands precursor Th17 cells with heightened stemness and antitumor activity. *JCI Insight* **2**, 90547 (2017).
64. L. Xu, Q. Huang, H. Wang, Y. Hao, Q. Bai, J. Hu, Y. Li, P. Wang, X. Chen, R. He, B. Li, X. Yang, T. Zhao, Y. Zhang, Y. Wang, J. Ou, H. Liang, Y. Wu, X. Zhou, L. Ye, The kinase mTORC1 promotes the generation and suppressive function of follicular regulatory T cells. *Immunity* **47**, 538–551.e5 (2017).
65. J. Yang, X. Lin, Y. Pan, J. Wang, P. Chen, H. Huang, H.-H. Xue, J. Gao, X.-P. Zhong, Critical roles of mTOR Complex 1 and 2 for T follicular helper cell differentiation and germinal center responses. *eLife* **5**, e17936 (2016).
66. M. K. Slifka, R. Ahmed, Long-term antibody production is sustained by antibody-secreting cells in the bone marrow following acute viral infection. *Ann. N. Y. Acad. Sci.* **797**, 166–176 (1996).
67. M. K. Slifka, M. Matloubian, R. Ahmed, Bone marrow is a major site of long-term antibody production after acute viral infection. *J. Virol.* **69**, 1895–1902 (1995).
68. M. K. Slifka, R. Antia, J. K. Whitmire, R. Ahmed, Humoral immunity due to long-lived plasma cells. *Immunity* **8**, 363–372 (1998).
69. F. M. Ndungu, E. T. Cadman, J. Coulcher, E. Nduati, E. Couper, D. W. MacDonald, D. Ng, J. Langhorne, Functional memory B cells and long-lived plasma cells are generated after a single *Plasmodium chabaudi* infection in mice. *PLOS Pathog.* **5**, e1000690 (2009).
70. J. J. Taylor, K. A. Pape, M. K. Jenkins, A germinal center–independent pathway generates unswitched memory B cells early in the primary response. *J. Exp. Med.* **209**, 597–606 (2012).
71. D. Butt, T. D. Chan, K. Bourne, J. R. Hermes, A. Nguyen, A. Statham, L. A. O'Reilly, A. Strasser, S. Price, P. Schofield, D. Christ, A. Basten, C. S. Ma, S. G. Tangye, T. G. Phan, V. K. Rao, R. Brink, FAS inactivation releases unconventional germinal center B cells that escape antigen control and drive IgE and autoantibody production. *Immunity* **42**, 890–902 (2015).
72. A. T. Krishnamurty, C. D. Thouvenel, S. Portugal, G. J. Keitany, K. S. Kim, A. Holder, P. D. Crompton, D. J. Rawlings, M. Pepper, Somatically hypermutated *plasmodium*-specific IgM^+ memory B cells are rapid, plastic, early responders upon malaria rechallenge. *Immunity* **45**, 402–414 (2016).
73. Q. P. Nguyen, T. Z. Deng, D. A. Witherden, A. W. Goldrath, Origins of $CD4^+$ circulating and tissue-resident memory T-cells. *Immunology* **157**, 3–12 (2019).
74. J. P. Weber, F. Fuhrmann, R. K. Feist, A. Lahmann, M. S. Al Baz, L.-J. Gentz, D. Vu van, H. W. Mages, C. Haftmann, R. Riedel, J. R. Grün, W. Schuh, R. A. Kroczek, A. Radbruch, M.-F. Mashreghi, A. Hutloff, ICOS maintains the T follicular helper cell phenotype by down-regulating Krüppel-like factor 2. *J. Exp. Med.* **212**, 217–233 (2015).
75. A. O. Moguche, S. Shafiani, C. Clemons, R. P. Larson, C. Dinh, L. E. Higdon, C. J. Cambier, J. R. Sissons, A. M. Gallegos, P. J. Fink, K. B. Urdahl, ICOS and Bcl6-dependent pathways maintain a CD4 T cell population with memory-like properties during tuberculosis. *J. Exp. Med.* **212**, 715–728 (2015).
76. G. R. Bantug, L. Galluzzi, G. Kroemer, C. Hess, The spectrum of T cell metabolism in health and disease. *Nat. Rev. Immunol.* **18**, 19–34 (2018).
77. K. Araki, A. P. Turner, V. O. Shaffer, S. Gangappa, S. A. Keller, M. F. Bachmann, C. P. Larsen, R. Ahmed, mTOR regulates memory CD8 T-cell differentiation. *Nature* **460**, 108–112 (2009).
78. E. L. Pearce, M. C. Walsh, P. J. Cejas, G. M. Harms, H. Shen, L.-S. Wang, R. G. Jones, Y. Choi, Enhancing CD8 T-cell memory by modulating fatty acid metabolism. *Nature* **460**, 103–107 (2009).
79. L. Ye, J. Lee, L. Xu, A.-U.-R. Mohammed, W. Li, J. S. Hale, W. G. Tan, T. Wu, C. W. Davis, R. Ahmed, K. Araki, mTOR promotes antiviral humoral immunity by differentially regulating CD4 helper T cell and B cell responses. *J. Virol.* **91**, e01653-16 (2017).
80. Y. Maekawa, C. Ishifune, S.-i. Tsukumo, K. Hozumi, H. Yagita, K. Yasutomo, Notch controls the survival of memory $CD4^+$ T cells by regulating glucose uptake. *Nat. Med.* **21**, 55–61 (2015).
81. A. T. Phan, A. L. Doedens, A. Palazon, P. A. Tyrakis, K. P. Cheung, R. S. Johnson, A. W. Goldrath, Constitutive glycolytic metabolism supports $CD8^+$ T cell effector memory differentiation during viral infection. *Immunity* **45**, 1024–1037 (2016).
82. S. Dimeloe, M. Mehling, C. Frick, J. Loeliger, G. R. Bantug, U. Sauder, M. Fischer, R. Belle, L. Develioglu, S. Tay, A. Langenkamp, C. Hess, The immune-metabolic basis of effector memory $CD4^+$ T cell function under hypoxic conditions. *J. Immunol.* **196**, 106–114 (2016).
83. A. F. Ochsenbein, D. D. Pinschewer, S. Sierro, E. Horvath, H. Hengartner, R. M. Zinkernagel, Protective long-term antibody memory by antigen-driven and T help-dependent differentiation of long-lived memory B cells to short-lived plasma cells independent of secondary lymphoid organs. *Proc. Natl. Acad. Sci. U.S.A.* **97**, 13263–13268 (2000).
84. S. G. Tangye, Staying alive: Regulation of plasma cell survival. *Trends Immunol.* **32**, 595–602 (2011).
85. L.-H. Thai, S. Le Gallou, A. Robbins, E. Crickx, T. Fadeev, Z. Zhou, N. Cagnard, J. Mégret, C. Bole, J.-C. Weill, C.-A. Reynaud, M. Mahévas, BAFF and $CD4^+$ T cells are major survival factors for long-lived splenic plasma cells in a B-cell–depletion context. *Blood* **131**, 1545–1555 (2018).

86. J. Shi, S. Hou, Q. Fang, X. Liu, X. Liu, H. Qi, PD-1 controls follicular T helper cell positioning and function. *Immunity* **49**, 264–274.e4 (2018).
87. L. L. Teichmann, J. L. Cullen, M. Kashgarian, C. Dong, J. Craft, M. J. Shlomchik, Local triggering of the ICOS coreceptor by CD11c$^+$ myeloid cells drives organ inflammation in lupus. *Immunity* **42**, 552–565 (2015).
88. E. Hammarlund, A. Thomas, I. J. Amanna, L. A. Holden, O. D. Slayden, B. Park, L. Gao, M. K. Slifka, Plasma cell survival in the absence of B cell memory. *Nat. Commun.* **8**, 1781 (2017).
89. S. A. Valkenburg, O. T. W. Li, A. Li, M. Bull, T. A. Waldmann, L. P. Perera, M. Peiris, L. L. M. Poon, Protection by universal influenza vaccine is mediated by memory CD4 T cells. *Vaccine* **36**, 4198–4206 (2018).
90. D. T. Utzschneider, M. Charmoy, V. Chennupati, L. Pousse, D. P. Ferreira, S. Calderon-Copete, M. Danilo, F. Alfei, M. Hofmann, D. Wieland, S. Pradervand, R. Thimme, D. Zehn, W. Held, T cell factor 1-expressing memory-like CD8$^+$ T cells sustain the immune response to chronic viral infections. *Immunity* **45**, 415–427 (2016).
91. J. B. Wing, Y. Kitagawa, M. Locci, H. Hume, C. Tay, T. Morita, Y. Kidani, K. Matsuda, T. Inoue, T. Kurosaki, S. Crotty, C. Coban, N. Ohkura, S. Sakaguchi, A distinct subpopulation of CD25$^-$ T-follicular regulatory cells localizes in the germinal centers. *Proc. Natl. Acad. Sci. U.S.A.* **114**, E6400–E6409 (2017).
92. J. Q. Wu, M. Seay, V. P. Schulz, M. Hariharan, D. Tuck, J. Lian, J. Du, M. Shi, Z. Ye, M. Gerstein, M. P. Snyder, S. Weissman, Tcf7 is an important regulator of the switch of self-renewal and differentiation in a multipotential hematopoietic cell line. *PLOS Genet.* **8**, e1002565 (2012).
93. M. Battegay, Quantification of lymphocytic choriomeningitis virus with an immunological focus assay in 24 well plates. *ALTEX* **10**, 6–14 (1993).
94. J. J. Moon, H. H. Chu, J. Hataye, A. J. Pagán, M. Pepper, J. B. McLachlan, T. Zell, M. K. Jenkins, Tracking epitope-specific T cells. *Nat. Protoc.* **4**, 565–581 (2009).
95. R. Sommerstein, L. Flatz, M. M. Remy, P. Malinge, G. Magistrelli, N. Fischer, M. Sahin, A. Bergthaler, S. Igonet, J. ter Meulen, D. Rigo, P. Meda, N. Rabah, B. Coutard, T. A. Bowden, P.-H. Lambert, C.-A. Siegrist, D. D. Pinschewer, Arenavirus glycan shield promotes neutralizing antibody evasion and protracted infection. *PLOS Pathog.* **11**, e1005276 (2015).
96. O. Schweier, U. Aichele, A.-F. Marx, T. Straub, J. S. Verbeek, D. D. Pinschewer, H. Pircher, Residual LCMV antigen in transiently CD4$^+$ T cell-depleted mice induces high levels of virus-specific antibodies but only limited B-cell memory. *Eur. J. Immunol.* **49**, 626–637 (2019).
97. M. E. Ritchie, B. Phipson, D. Wu, Y. Hu, C. W. Law, W. Shi, G. K. Smyth, *limma* powers differential expression analyses for RNA-sequencing and microarray studies. *Nucleic Acids Res.* **43**, e47 (2015).
98. A. Liberzon, A. Subramanian, R. Pinchback, H. Thorvaldsdottir, P. Tamayo, J. P. Mesirov, Molecular signatures database (MSigDB) 3.0. *Bioinformatics* **27**, 1739–1740 (2011).
99. A. Subramanian, P. Tamayo, V. K. Mootha, S. Mukherjee, B. L. Ebert, M. A. Gillette, A. Paulovich, S. L. Pomeroy, T. R. Golub, E. S. Lander, J. P. Mesirov, Gene set enrichment analysis: A knowledge-based approach for interpreting genome-wide expression profiles. *Proc. Natl. Acad. Sci. U.S.A.* **102**, 15545–15550 (2005).
100. S. Aibar, C. B. González-Blas, T. Moerman, V. A. Huynh-Thu, H. Imrichova, G. Hulselmans, F. Rambow, J.-C. Marine, P. Geurts, J. Aerts, J. van den Oord, Z. K. Atak, J. Wouters, S. Aerts, SCENIC: Single-cell regulatory network inference and clustering. *Nat. Methods* **14**, 1083–1086 (2017).
101. M. R. Corces, A. E. Trevino, E. G. Hamilton, P. G. Greenside, N. A. Sinnott-Armstrong, S. Vesuna, A. T. Satpathy, A. J. Rubin, K. S. Montine, B. Wu, A. Kathiria, S. W. Cho, M. R. Mumbach, A. C. Carter, M. Kasowski, L. A. Orloff, V. I. Risca, A. Kundaje, P. A. Khavari, T. J. Montine, W. J. Greenleaf, H. Y. Chang, An improved ATAC-seq protocol reduces background and enables interrogation of frozen tissues. *Nat. Methods* **14**, 959–962 (2017).
102. S. K. Denny, D. Yang, C.-H. Chuang, J. J. Brady, J. S. Lim, B. M. Grüner, S.-H. Chiou, A. N. Schep, J. Baral, C. Hamard, M. Antoine, M. Wislez, C. S. Kong, A. J. Connolly, K.-S. Park, J. Sage, W. J. Greenleaf, M. M. Winslow, Nfib promotes metastasis through a widespread increase in chromatin accessibility. *Cell* **166**, 328–342 (2016).
103. A. Dobin, C. A. Davis, F. Schlesinger, J. Drenkow, C. Zaleski, S. Jha, P. Batut, M. Chaisson, T. R. Gingeras, STAR: Ultrafast universal RNA-seq aligner. *Bioinformatics* **29**, 15–21 (2013).
104. Y. Liao, G. K. Smyth, W. Shi, The R package *Rsubread* is easier, faster, cheaper and better for alignment and quantification of RNA sequencing reads. *Nucleic Acids Res.* **47**, e47 (2019).
105. P. M. Gubser, G. R. Bantug, L. Razik, M. Fischer, S. Dimeloe, G. Hoenger, B. Durovic, A. Jauch, C. Hess, Rapid effector function of memory CD8$^+$ T cells requires an immediate-early glycolytic switch. *Nat. Immunol.* **14**, 1064–1072 (2013).

Acknowledgments: We thank D. Pinschewer for many helpful discussions, sharing reagents, and technical advice; M. Linterman for critical reading of the manuscript; G. Bantug and D. Labes for expertise and discussion; C. Beisel for technical advice; R. Tussiwand and her lab for feedback and support; T. Rezzonico and F. Grassi for technical support, the flow sorting facility, and all the animal caretakers at the DBM University of Basel. scRNA-seq was performed at the Genomics Facility Basel, ETH Zurich. Calculations were performed at sciCORE (http://scicore.unibas.ch/) scientific computing center at the University of Basel.
Funding: Supported by research grants to C.G.K. (SNF PP00P3_157520, Gottfried and Julia Bangerter-Rhyner Stiftung, Olga Mayenfisch Stiftung, and Swiss Life Jubiläumsstiftung).
Author contributions: M.K., D.S., and C.G.K. conceptualized the project. M.K., D.S., and C.G.K. designed the experiments. M.K., T.C.P., C.G.K., J.L., N.S., and L.C.L. performed experiments. Y.I.E. (recombinant NP) and R.P.J. (NICD protector) produced reagents. M.K., D.S., C.G.K., J.R., and F.G. analyzed the data. C.G.K., D.S., and M.K. wrote the manuscript. M.K., D.S., and C.G.K. visualized the data. C.G.K. acquired funding. J.J.T., C.H., and T.M. provided resources. C.G.K. supervised the study. **Competing interests:** The authors declare that they have no competing interests. **Data and materials availability:** The scRNA-seq, bulk RNA-seq, and ATAC-seq data have been deposited in the National Center for Biotechnology Information Gene Expression Omnibus database (accession number: SuperSeries GSE139198). NIP-transgenic mice were generated in the lab of S. Crotty. Requests for this strain should be addressed to S. Crotty (shane@lji.org).

Submitted 30 August 2019
Accepted 16 January 2020
Published 6 March 2020
10.1126/sciimmunol.aay5552

Citation: M. Künzli, D. Schreiner, T. C. Pereboom, N. Swarnalekha, L. C. Litzler, J. Lötscher, Y. I. Ertuna, J. Roux, F. Geier, R. P. Jakob, T. Maier, C. Hess, J. J. Taylor, C. G. King, Long-lived T follicular helper cells retain plasticity and help sustain humoral immunity. *Sci. Immunol.* **5**, eaay5552 (2020).

Science Immunology

Long-lived T follicular helper cells retain plasticity and help sustain humoral immunity

Marco KünzliDavid SchreinerTamara C. PereboomNivedya SwarnalekhaLudivine C. LitzlerJonas LötscherYusuf I. ErtunaJulien RouxFlorian GeierRoman P. JakobTimm MaierChristoph HessJustin J. TaylorCarolyn G. King

Sci. Immunol., 5 (45), eaay5552. • DOI: 10.1126/sciimmunol.aay5552

Memory Tfh cells

Expression of a purinergic receptor P2X7R renders certain T cell subsets, including resident memory T (T) cells susceptible to NAD-induced cell death (NICD). Injection of an NICD protector before harvesting them improves cell recovery. Here, based on the observation that T follicular helper (T) cells also express P2X7R, Künzli *et al.* used NICD protector to study the persistence of T cells after LCMV infection in mice. They report that T cells persisted for 400+ days after infection and that long-lived T cells are glycolytic and are marked by high expression of folate receptor 4 (FR4). Upon reinfection, these FR4 “memory” T cells were capable of self-renewal and could also give rise to effector and central memory cells.

Science Immunology (ISSN 2470-9468) is published by the American Association for the Advancement of Science. 1200 New York Avenue NW, Washington, DC 20005. The title *Science Immunology* is a registered trademark of AAAS.